PRODUCTION AND CHARACTERISATION OF POLY(L-LACTIC ACID)/GRAPHENE OXİDE NANOFIBERS FOR NERVE REGENERATION

by

Hayriye Öztatlı

B.S., Chemical Engineering, Yeditepe University, 2012

B.S., Industrial and System Engineering, Yeditepe University, 2013

Submitted to the Institute of Biomedical Engineering

in partial fulfillment of the requirements

for the degree of

Master of Science

in

Biomedical Engineering

Boğaziçi University

2016

PRODUCTION AND CHARACTERISATION OF POLY(L-LACTIC ACID)/GRAPHENE OXİDE NANOFIBERS FOR NERVE REGENERATION

APPROVED BY:

Assist. Prof. Dr. Duygu Ege .....
(Thesis Advisor)

Assoc. Prof. Dr. Bora Garipcan .....

Assist. Prof. Dr. Sinan Yıldırım .....

DATE OF APPROVAL: 12 August 2016

ACKNOWLEDGEMENTS

I would like to express the profound gratitude and special thanks to my advisor Assist. Prof. Dr. Duygu Ege for her constructive guidance, advice and supervision on this thesis.

I am grateful to Assoc. Prof. Dr. Bora Garipcan and his laboratory members for their supports. Also, I would like to deeply thank my committee member Assist. Prof. Dr. Sinan Yıldırım.

I would like to thank Boğaziçi University Scientific Research Fund (BAP) for the financial support under project number 9940.

There are no words that can express my appreciation to my family for their support, dedication, love and persistent confidence in me truly. Also, I specially thank Sabra Rostami, Hatice Kaya, Sedef Yusufoğulları, Deniz Kılınç, Öznur Demir, Ayşe Sena Sarp and all my laboratory group members for their moral support, motivation and everything we have shared together.

This thesis would not have come true without the contributions of so many people whose names could not be enumerated one by one individually, whom I would like to sincerely acknowledge their contributions.

ACADEMIC ETHICS AND INTEGRITY STATEMENT

I, Hayriye Öztatlı, hereby certify that I am aware of the Academic Ethics and Integrity Policy issued by the Council of Higher Education (YÖK) and I fully acknowledge all the consequences due to its violation by plagiarism or any other way.

Name :

Signature:

Date:

ABSTRACT

PRODUCTION AND CHARACTERISATION OF POLY(L-LACTIC ACID)/GRAPHENE OXİDE NANOFIBERS FOR NERVE REGENERATION

The development of biodegradable polymeric nanofiber scaffolds for a potential effort to repair injured nerve cells attracts great interest in nerve tissue engineering field. Poly (L-lactic acid) (PLLA) has being widely used in development of nerve fiber studies due to its biocompatibility, easily shaped properties and degradation to low toxic lactic acid. However, its hydrophobicity and lack of binding sites for cellular activities restricts its use as implants. In this regard, this study involves the incorporation of Graphene Oxide (GO) into PLLA either electrospun GO with PLLA or coating GO onto the PLLA and PLLA/GO nanofibers to fabricate ideal scaffolds with appropriate physical, mechanical and chemical properties of nanofiber mimicking the properties of the peripheral nerve. Hence, PLLA and PLLA/GO nanofibers were prepared via processing PLLA and PLLA/GO solutions with electrospinning and solution parameters (the concentration of PLLA, GO ratio and composition of binary system) were optimized to obtain thin and bead free nanofibers. Then, the fabricated nanofibers were functionalized with 1,6-Hexamethylenediamine (HMDA) and then coated with GO sheets. The fabricated PLLA, PLLA/GO and GO coated PLLA and PLLA/GO nanofibers were characterized via Light Microscopy, Scanning Electron Microscopy (SEM), Raman Spectroscopy, Ninhydrin assay, X-Ray Photoelectron Spectroscopy (XPS), tensile test and Water Contact Angle (WCA) measurement. The characterization results revealed that addition of GO either as filler or coating material enhanced physical, mechanical and chemical properties of nanofiber scaffold. In conclusion, the developed nanofiber scaffolds are promising for possible nerve regeneration application.

Keywords: Poly (L-lactic acid) (PLLA), Graphene Oxide (GO), 1,6-Hexamethylenediamine (HMDA), Nerve Regeneration

ÖZET

ÇEVRESEL SİNİR REJENERASYONU İÇİN POLİ(L-LAKTİK ASİT)/GRAFEN OKSİT NANOLİFLERİNİN ÜRETİLMESİ VE KARAKTERİZASYONU

Hasar görmüş sinir hücrelerini onarabilme yeteneğine sahip biyobozunan polimerik nanolif iskelelerinin geliştirilmesi sinir mühendisliği alanında büyük ilgi çekmektedir. Poli (L-laktik asit)(PLLA) biyouyumluluğu, kolay şekillendirilmesi, ve az toksik olan laktik asite bozunmasından dolayı sinir fiberi geliştiren çalışmalarda yaygın olarak kullanılmıştır. Fakat, hidrofobikliği ve hücresel aktiviteler için bağlanma gruplarının yeterli olmaması implant olarak kullanılmasını kısıtlar. Bu bağlamda, fiziksel, kimyasal ve mekanik özelliklere uygun çevresel sinirlerin özelliklerini taklit eden ideal iskeleri üretmek için bu çalışma Grafen Oksit (GO) ya PLLA içine eklenerek eğrilmesi veya GO'nın nanolif iskelelerinin yüzeylerine kaplanmasını içerir. Böylelikle, PLLA/GO ve PLLA nanolifleri PLLA ve PLLA/GO çözeltilerinin elektroeğirme ile işlenerek üretilmiştir ve boncuk yapıların olmadığı, ince nanoliflerin elde edilmesi için çözelti parametreleri (PLLA konsantrasyonu, GO oranı ve ikili çözücünün bileşimi) optimize edilmiştir. Ardından üretilen PLLA/GO ve PLLA nanolifleri 1,6 heksametilendiamin (HMDA) ile fonksiyonlaştırılmış ve daha sonra GO ile kaplanmışlardır. Üretilen PLLA, PLLA/GO ve GO ile kaplamış PLLA ve PLLA/GO nanolifler Isık Mikroskobu, Taramalı Elektron Mikroskobu (SEM), Raman Spektroskopi, ninhidrin boyama, X-ışını Fotoelectron Spektroskopisi, çekme testi ve Su Temas Açısı karakterizasyon yöntemleri ile karakterize edilmiştir. Karakterizasyon sonuçları, GO'nun dolgu ya da kaplama malzemesi olarak kullanılması nanolif iskelelerinin fiziksel, mekanik ve kimyasal özelliklerini geliştirmiştir. Sonuç olarak, geliştirilen nanolif iskeleleri olası sinir rejenerasyonu uygulaması için umut vericidir.

Anahtar Sözcükler: Poli (L-laktik asit) (PLLA), Grafen Oksit (GO), 1,6 heksametilendiamin (HMDA), Sinir rejenerasyonu

TABLE OF CONTENTS

LIST OF FIGURES

LIST OF TABLES

LIST OF SYMBOLS

LIST OF ABBREVIATIONS

Chl	Chloroform
CNS	Central Nervous System
DMF	N,N- DimethylFormamide
ECM	Extracellular Matrix
FLG	Few Layered Graphene
GNS	Graphene Nanosheets
GO	Graphene Oxide
HMDA	1,6 Hexamethylenediamine
IPA	Isopropanol
NSC	Neural Stem Cells
PCL	Polycaprolactone
PGA	Poly(glycolic Acid)
PLLA	Poly (L-Lactic Acid)
PNS	Peripheral Nervous System
rGO	Reduced Graphene Oxide
SC	Schwann Cells
SEM	Scanning Electron Microscopy
UTS	Ultimate Tensile Strength
UV-VIS	Ultraviolet Visible
WCA	Water Contact Angle
XPS	X-Ray Photoelectron Spectroscopy

1. INTRODUCTION

1.1 Motivation

Peripheral nerve injury is a serious global medical and public health problem and significantly affects the patients' quality of life [1, 2]. Short gap of the peripheral nerve damage recover very slowly and if the gap between transected nerve ends is large, self- recovery becomes impossible [3]. Hence, repair and regeneration strategies of peripheral nerve injuries have taken a great deal of consideration.

Currently there are a variety of treatment techniques including direct repair, autograft and allograft. Autografts are considered as the gold standard technique to repair nerve injuries, however they have substantial limitations such as insufficiency of donor nerves particularly for recovery of long nerve lesions, high risk of unsuccessful transplantation and poor functional recovery. All in all, these limitations have encouraged the development of alternative approaches for repair and regeneration of peripheral nerve that gives the best results with great consistency [2, 4, 5].

Recently, advances in nanotechnology and tissue engineering that have incorporated with neuroscience have developed an optimistic future to improve nerve regeneration strategies [4]. Researches in neural tissue engineering field have attempted to develop synthetic scaffolds that mimic structural and biological properties of the natural extracellular matrix and can support three dimensional cell cultures to allow cells to proliferate and migrate [1, 6].

The development of scaffolds with defined properties to guide Schwann cells (SCs) to repair and regenerate injured nerve is still in its infancy. The interaction of cells with their neighboring cells, the surrounding fluid and extracellular matrix (ECM) is mainly based on chemical and physical cues provided by the scaffolds. Hereof, electrospun scaffolds with properties of high surface to volume ratio, morphological

resembles to the fibers existing in human body and high porosity and roughness provide ideal topography for the regeneration of nerve [7].

Poly (L-Lactic Acid) (PLLA) is a biocompatible and bioresorbable synthetic polymer [8]. The use of the PLLA in tissue engineering applications attracts noteworthy interests because it degrades to lactic acid that can be removed from body as carbon dioxide and water [9]. However, PLLA scaffolds do not have cell recognition sites and depending on this it hinders cell attachment and other cellular behaviors [**?**]. Hence, in order to fabricate ideal scaffolds from PLLA for nerve tissue engineering application, it needs to be incorporated with biologically active materials.

Graphene based nanomaterials specifically graphene oxide (GO) has been considered as a novel nanomaterial for designing neural scaffolds due to biocompatibility and its special characteristic such as unique surface chemistry, high affinity for water, high mechanical properties and high conductivity to facilitate electrical stimulation of nerves. In particular, GO provides chemical cues by its oxygen containing groups that help to organize and direct cellular behavior [10]. Therefore, the use of the GO in combination with PLLA in electrospun scaffolds promote remarkable improvement in the properties of the materials for nerve regeneration applications [11].

Recently a number of researches have been conducted to investigate physical, chemical and biological activity of electrospun scaffolds containing graphene based nanomaterials. Among these studies, Shah et. al examined the effect of dip coating of Polycaprolacton (PCL) fibers with GO on neural stem cell (NSC) differentiation. The results of the study have shown that while electrospinning process provided an ideal surface topography, GO promoted chemical (cell recognition sites) and physical cues (conductive and permissive surface) for differentiation of neural stem cells [12].

In another study, Chaudhuri et al. analyzed the differentiation of human cord blood derived mesenchymal stem cells (CB-hMSCs) to skeletal muscle cells (hSkMCs) on spin coated thin GO sheets and on electrospun fibrous meshes of GO/PCL composite. This study revealed that the addition of GO in bioactive polymer improved its

conductivity, dielectric permittivity along with biocompatibility. Therefore, GO/PCL promoted better supporting cues for the formation of highly oriented multi-nucleated myotubes on the electrospun meshes compared to the GO sheets [13].

Additionally, Zhang et al. examined the effect of incorporation of GO and pegylated GO (surface of GO grafted with poly (ethylene glycol)) (GO-g-PEG) into poly (lactic acid) (PLA) on thermal, mechanical, wettability properties and cytocompatibility with Swiss mouse NIH 3T3 cells. Results revealed that thermal, mechanical and wettability properties of scaffolds enhanced with the addition of GO-g-PEG into PLA. Also, the improved cytocompatibility, PLA/GO-g-PEG composite nanofiber is a promising scaffold to be used for tissue engineering [14].

These studies sparked an inspiration of the development of the novel neural scaffolds by combining the properties of GO with PLLA nanofiber to enhance physical, chemical and biological properties of currently used scaffolds.

1.2 Objective

The hypothesis of this study was that incorporation of GO into PLLA structure as reinforcement or coating material improves the properties of PLLA nanofiber scaffolds that would be suitable for possible nerve regeneration applications.

The main objectives of this study are as follows:

1. To investigate the reinforcement effect of GO concentration on physical, chemical, mechanical and conductive properties of PLLA nanofibers.
2. To examine the coating effect of GO on chemical, mechanical and conductive properties of PLLA.
3. To analyze both reinforcement and coating effect of GO on the properties of PLLA.

1.3 Outline

This thesis begins with a background chapter that includes general information about nervous system, peripheral nerve injury, nerve tissue engineering, biomaterials and techniques used to fabricate scaffolds. In the Chapter 2, materials selection and experimental procedures are explained in detail. After materials and methods section, experimental findings are presented, which will follow by related discussions of the obtained results are presented. Finally, some recommendations for the future work are given.

2. BACKGROUND

2.1 Nervous System

The nervous system is classified into the central nervous system (CNS) and peripheral nervous system (PNS) and they differ in their physiology and function. While CNS that comprises of spinal cord and brain, PNS consists of sensory and motor neurons [15]. One of the most striking differences between PNS and CNS is that unlike CNS nerve fibers, PNS nerve fibers can regenerate significantly once peripheral nerve is damaged. This distinction might be because of the inhibitory effect of oligodendroglia and the stimulatory effect of Schwann cells on axonal regeneration [16, 17].

In nervous system, different types of cells interact with each other to transmit signals around the brain and between the brain and body. These cells can be divided in neurons and neuroglia. Neurons are electrically excitable cells of the nervous system and comprised of a cell body (soma) and its extensions (axons and dendrites). However, glia cells are non-excitable neural cells that provide support for function of neurons and they consist astrocytes, oligodendroctyes and ependymal cells in CNS and Schwann cells (SCs) in PNS. Glial cells are more abundant than neurons and they have some capability of cell division whereas neuron cells do not divide [18, 19].

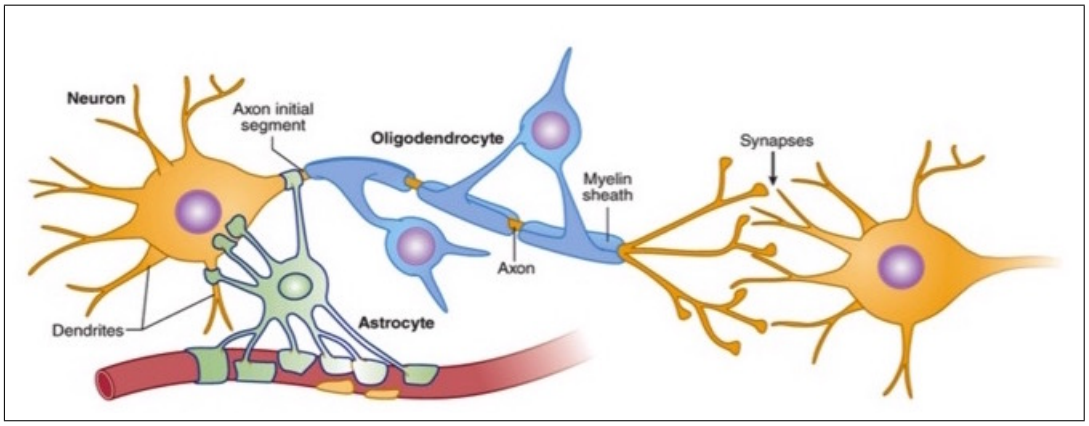

Figure 2.1 Central nervous system cell types [20]

2.2 Peripheral Nervous System

PNS has a complex structure and two important functions. Firstly, it collects information from external environment, converts it to nerve signals and carries it to the central nervous system. Secondly, it transmits information from CNS and processes it to be interpreted to the target organs.

The peripheral nerve involves nerve fiber and supportive tissue. Cell body is situated in either in spinal chord and spinal nerves or in the brain. Nerve fibers extend longitudinally from cell body to the surrounding and they have two main function. First one is providing mechanical support for nerve fibers to endure stretching and compression due to movement of body. Second one is providing trophic support for the fibers via blood vessels. The connective tissue is made up of three layers as shown in Figure 2.2 Epineurium is the outermost layer that surrounds the nerve and protects it from the external environment. Perineurium is a mechanically strong layer by which bundles of fibers are separated from each other. It consists of epithelium like cells and collagen fibers and forms the diffusion barrier between epineurium and endoneurium. The last layer, endonerium is composed of loose collagenous matrix surrounding the nerve fibers and ensuring further protection for nerve fibers to withstand mechanical forces. The endonerium comprise of Schwann cells, fibroblasts, endothelial-like cells, macrophages and mastocytes [18, 21].

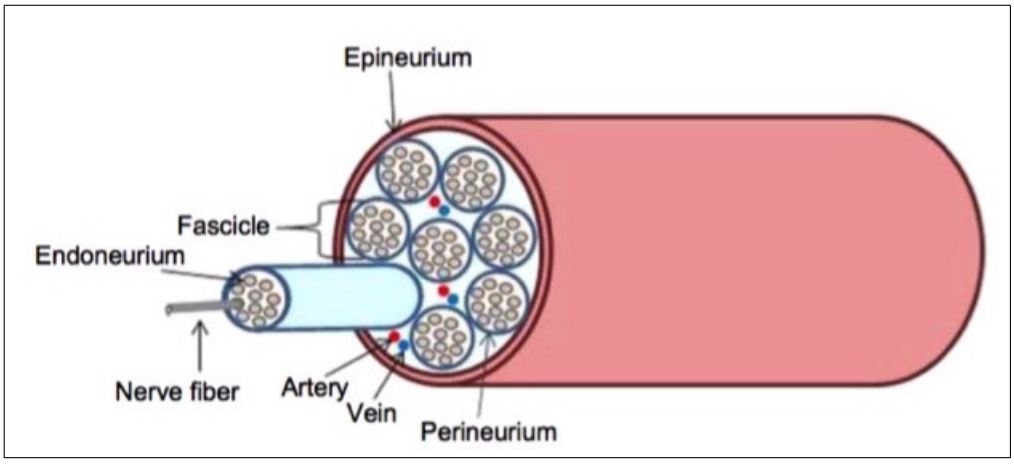

Figure 2.2 Peripheral nerve structure [22]

In PNS, nerve fibers exist as myelinated or unmyelinated and both of them are surrounded by SC that are responsible from supporting and myelinating the nerve fibers. In myelinated fibers, SCs form myelin sheaths that are connected by junctions, called as Nodes of Ranvier and it has important role in the fast saltatory conduction. However, slower conduction of the nerve pulse occurs in unmyelinated fibres [23, 24].

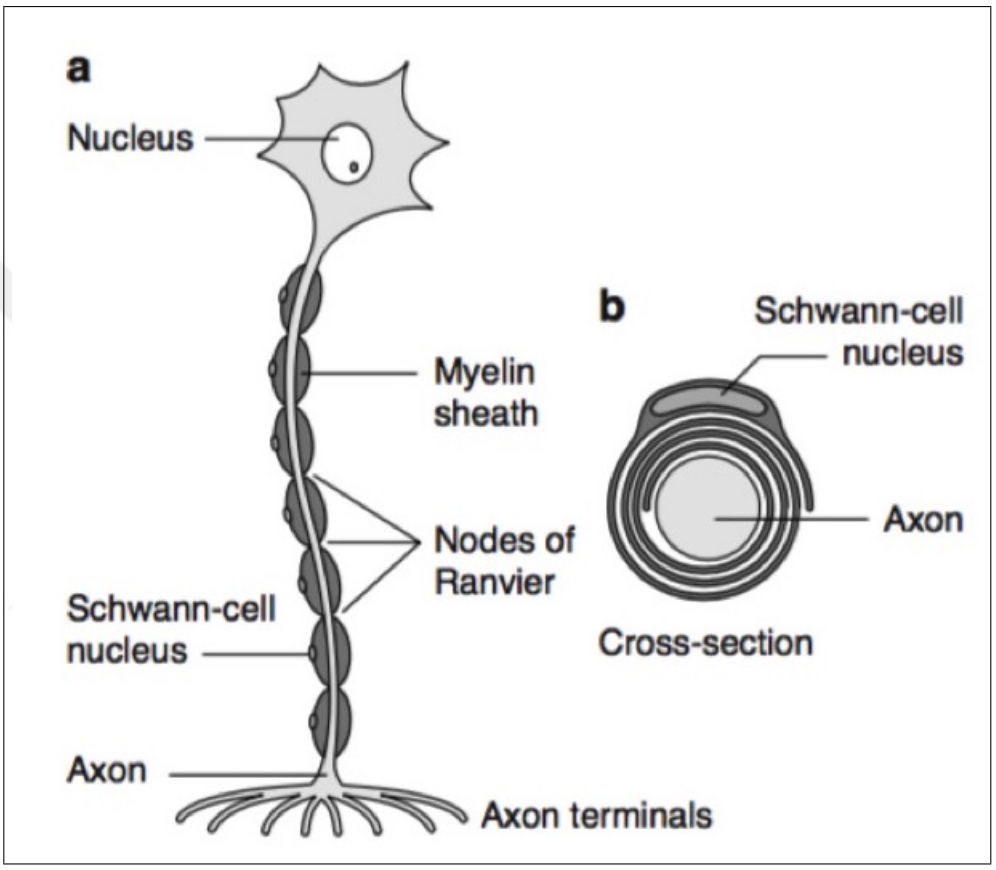

Figure 2.3 Peripheral nerve fiber and its cross section [15]

SCs also induce peripheral nerve regenerations through secreting neurotrophic factors, cell adhesion molecules and extracellular matrix components [24]. When a peripheral nerve injury is occurred, macrophages move to the distal stump of the injured nerves to clear debris of both myelin and axon released from the disintegration of nerve [25]. SCs proliferate and change from a myelinating to a regenerative phenotype. Through proliferation of SCs, Bands of Bungers, guiding the regrowing axons, is formed after Wallerian degeneration as shown in Figure 2.2 [21]. Activated SCs stimulate the prolongation of regenerating axons between two ends by secreting immunologically active substances [26].

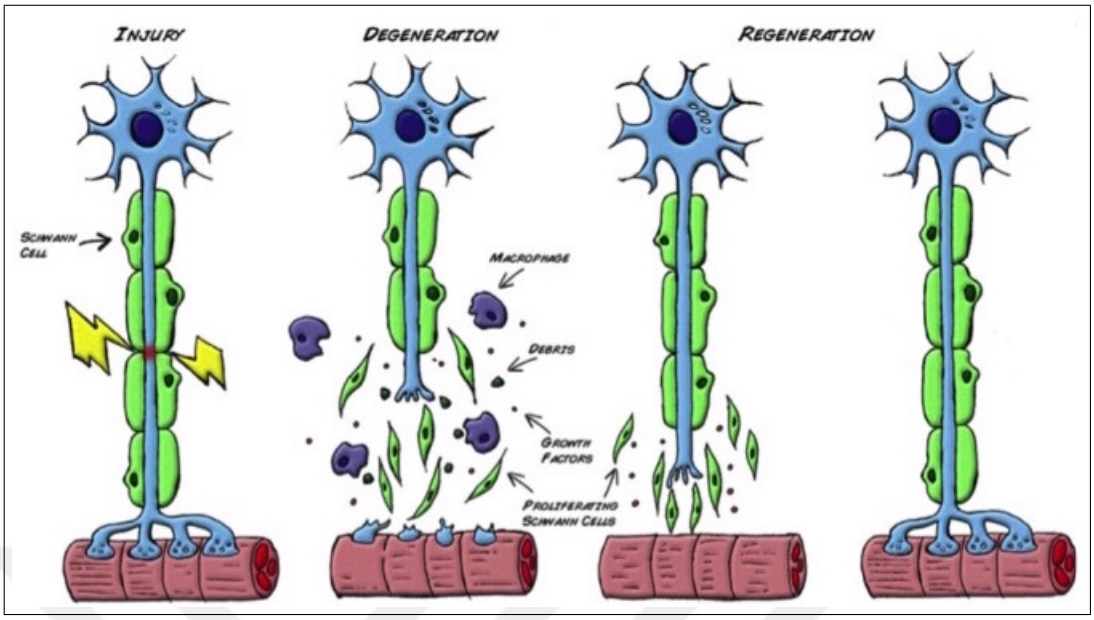

Figure 2.4 Wallerian degeneration of injured nerve [25]

2.3 Repair and Regeneration Strategies of PNS

When the nerve gap between transected nerve ends is large, regrowth of lost parts and reestablishment of the functional connection of stumps are impossible. Therefore, a device is implanted between the transected nerve ends to bridge the nerve ends and support axonal regrowth [1]. A wide range of nerve guide techniques has been explored for the treatment of nerve injuries as indicated in Figure 2.5.

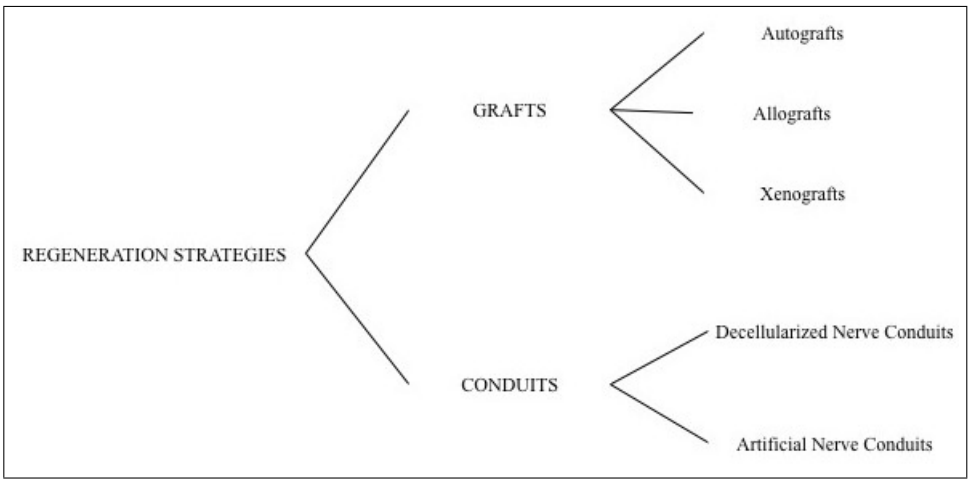

Figure 2.5 Regeneration strategies of nerve injury.

2.4 Nerve Grafts

Allografts, used to connect distal and proximal stumps with tissue derived a different individual of the same species, and xenografts, isolated from a member of another species, are used as a support for guidance of axonal regrowth [22]. However, they possess risk of disease transmission and infection in host tissue. Hence, the use of immunosuppression drugs is required, but in this case, long-term immune suppression leads to increase in risk of infections, decrease in healing rate and even tumor formation [22, 27].

Autologous graft, obtained from the same individual but from another part of the body, is considered as the gold standard technique to repair nerve injuries [28]. However, they have some limitations, namely shortage of donor nerves, particularly for recovery of several lengths of nerve lesions because it is self-donated nerve segment. In addition, mismatching between the donor site nerve size and the recipient site nerve size, tumor formation and fail of functional recovery are other restrictions [2, 3, 5].

2.5 Artificial Nerve Conduct

Currently, numerous researches have been conducted to develop artificial nerve made of biomaterials as an alternative for autologous nerve grafts [27]. These conduits are designed with a longitudinal shape in order to stimulate physicochemical and biological signals to direct formation of axons from proximal to distal end of neurons in order to reconnect them with one another. They also promote physical bridge for growth and avoid the infiltration of fibrous tissue into regenerated axon [26, 29].

The efficacy of a scaffold for substitution of an autologous nerve depends on whether they possess the optimum structural parameters to acquire restoration of nerve injury [28]. These parameters include:

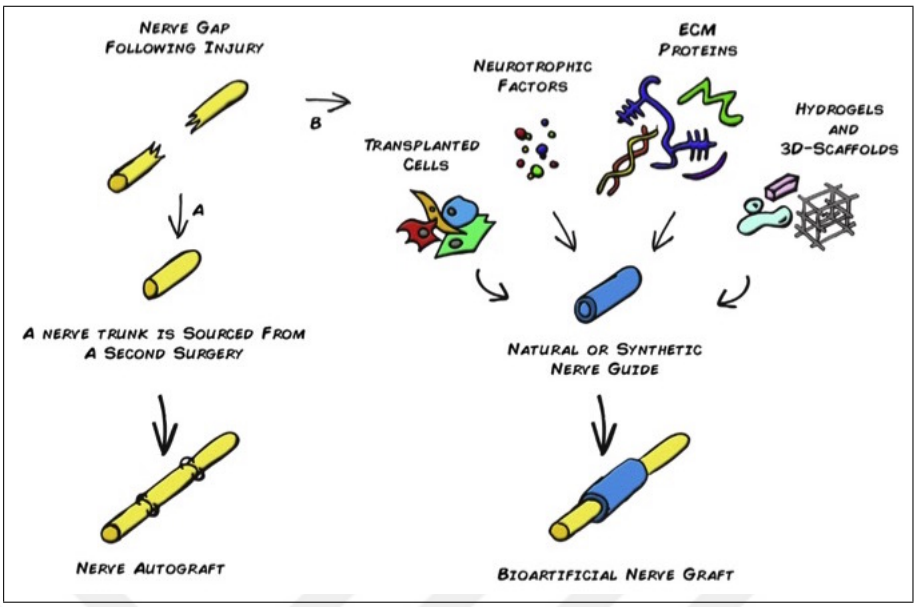

Figure 2.6 Peripheral nerve regeneration strategies a.) autograft b.) bioartificial nerve graft [25]

a) Biodegradability and biocompatibility of the material,

b) Non-toxicity and non-inflammatory,

c) Mechanical similarity to the intended site of implantation.

d) Possession of a large surface area and high porosity to provide more structural space for cell attachment and migration,

e) Interconnectivity and permeability from pores to favor nutrient and metabolic waste exchange between the scaffold and environment until the planted cells develop a new functional matrix,

f) Acting as a bridge to extend the regeneration axons into injury site and repair connections with the target innervation and promote functional recovery,

g) Appropriate surface chemistry to induce cellular attachment, differentiation and proliferation,

h) Ability to fabricated into a variety of shapes and sizes,

i) An easy and affordable fabrication process [6, 28].

Therefore, type of fabrication technique, and choice of biomaterial are critical parameters to produce an ideal neural scaffold [30].

2.6 Biomaterials for Neural Research

Biomaterial selection is considered to be a crucial parameter for the fabrication of neural scaffolds. When biomaterials are chosen for application of neural scaffolds, they must fulfill numerous physicochemical, biochemical and biological requirements. Therefore, a wide variety of natural polymers, synthetic biodegradable polymers and electric conducting materials have been examined as potential neural scaffold materials.

2.6.1 Natural Polymers

Naturally derived polymers, proteins and polysaccharides such as collagen, chitosan, alginate, fibrin and so on, have been used extensively for fabrication neural scaffold because neural scaffolds fabricated from natural biomaterials promise many attractive properties. These materials exhibit a very good biocompatibility, bioactivity, less toxic effects and great potential for clinical functionality. Most importantly, they contain biomolecular recognition sites that favor cell adhesion, migration, growth and proliferation of cells [31]. However, in addition to insufficiency of natural biomaterials, they have a tendency to denature or decompose at temperatures below their melting point, which leads to difficulties in the fabrication of scaffolds in different size and shape. Inducing natural polymers immunological reactions in a patient's body, high cost and batch to batch variability also limits their use in neural tissue engineering applications [32, 33].

2.6.2 Synthetic Polymers

Biodegradable synthetic polymers have been used as alternatives to natural polymers during fabrication neural scaffolds due to their wide available choices with biocompatibility, controllable biodegradability, adjustable mechanical strength properties not stimulate any immunological reactions and processability in different forms [22]. Synthetic materials also promote high porosity that favors cellular activities namely attachment, proliferation, migration and exchange of nutrient and metabolic wastes [34]. Aliphatic polyesters, including Poly (L- Lactic acid) (PLLA), Polycaproclactone (PCL), and Poly (glycolic acid) (PGA) are attracted particular attentions because they degrade to non-toxic products that can be metabolized and cleared from body and are approved by the US Food and Drug Administration for clinical application [33, 35]. PLLA is a biocompatible and bioabsorbable polymer and hydrolytic scission products of PLLA, lactic acid, is a natural metabolite of carbohydrate metabolism. These features of PLLA make it an ideal material for fabrication neural scaffolds [36].

2.6.3 Graphene and Graphene Based Materials

Graphene is comprised of sp^2 hybridized carbon atoms arranged hexagonally in two-dimensional crystal lattice. This structure provides it unique physical, chemical and mechanical properties [37]. This single atom thick nanomaterial exhibits large surface area, high stiffness, strong mechanical strength and electrical conductivity [11,37]. Graphene and its derivatives namely few layer graphenes (FLGs), graphene nanosheets (GNSs), graphene oxide (GO) and reduced graphene oxide (rGO) can be used as a biocompatible material for application of biomedical engineering [38].

Even though sp^2 hybridization of carbon atoms in graphene structure gives remarkable physical properties and it leads to the weak reactivity of graphene, restricting its use in engineering applications [40]. However, GO, oxidative form of graphene, possess unique chemical structures consisting of oxygen containing groups such as carboxyls, hydroxyls, epoxides and carbonyls. Oxygen containing groups facilitate sol-

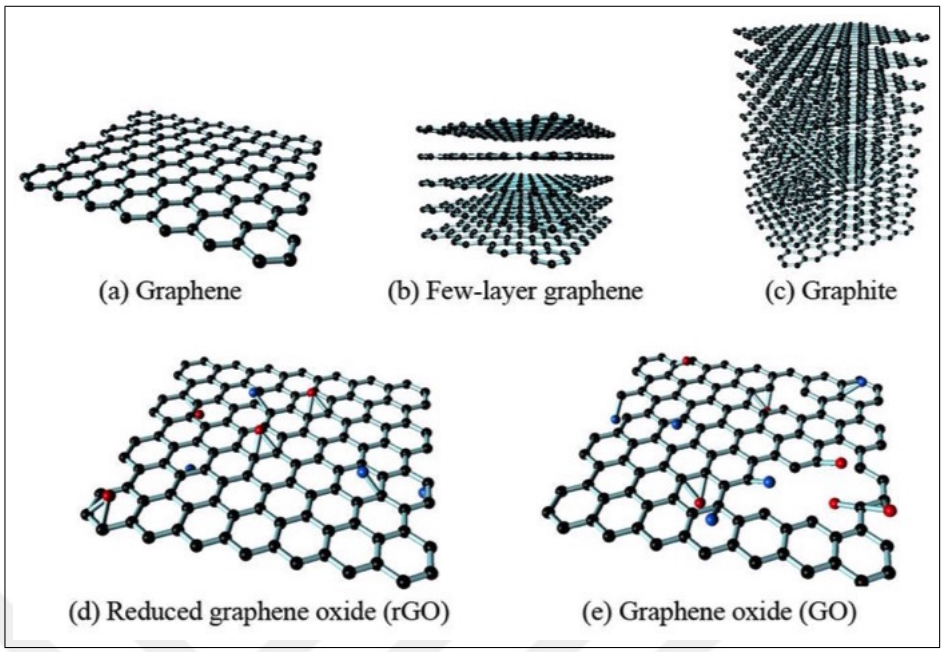

Figure 2.7 The structures of Graphene and its derivatives [39]

ubility in physiological conditions through formation of hydrogen bonds with water molecules. Specifically, carboxyl and hydroxyl groups facilitate interaction between surface and biomolecules or cells [10]. Hereby, they give exceptional advantages to GO for potential biomedical applications.

Graphene and its derivative based materials have emerged as novel material for biomedical applications such as drug and gene delivery, biosensor, imaging, tissue engineering and so on [42]. In particular, GO is considered as a distinctive material for application of tissue engineering. It can be used as ideal nanocarrier for drugs/genes owing to ability of physisorption and chemisorption of targets. In addition, GO materials exhibits excellent antimicrobial effect against wide range of microorganisms. Hence, recently many researches have been conducted to develop GO based anti-microbial scaffolds [43]. GO also have been used as substrate for the adhesion, proliferation and differentiation of numerous cell types due to reactivity of its hydrophilic groups and its aromatic groups that have ability of adsorption of natural extracellular matrix components [10]. Furthermore, electrical conductivity of GO has brought great advantages for use in nerve tissue engineering applications since it provides electrical stimulation to induce neurite outgrowth, which, in turn improves nerve regeneration [42].

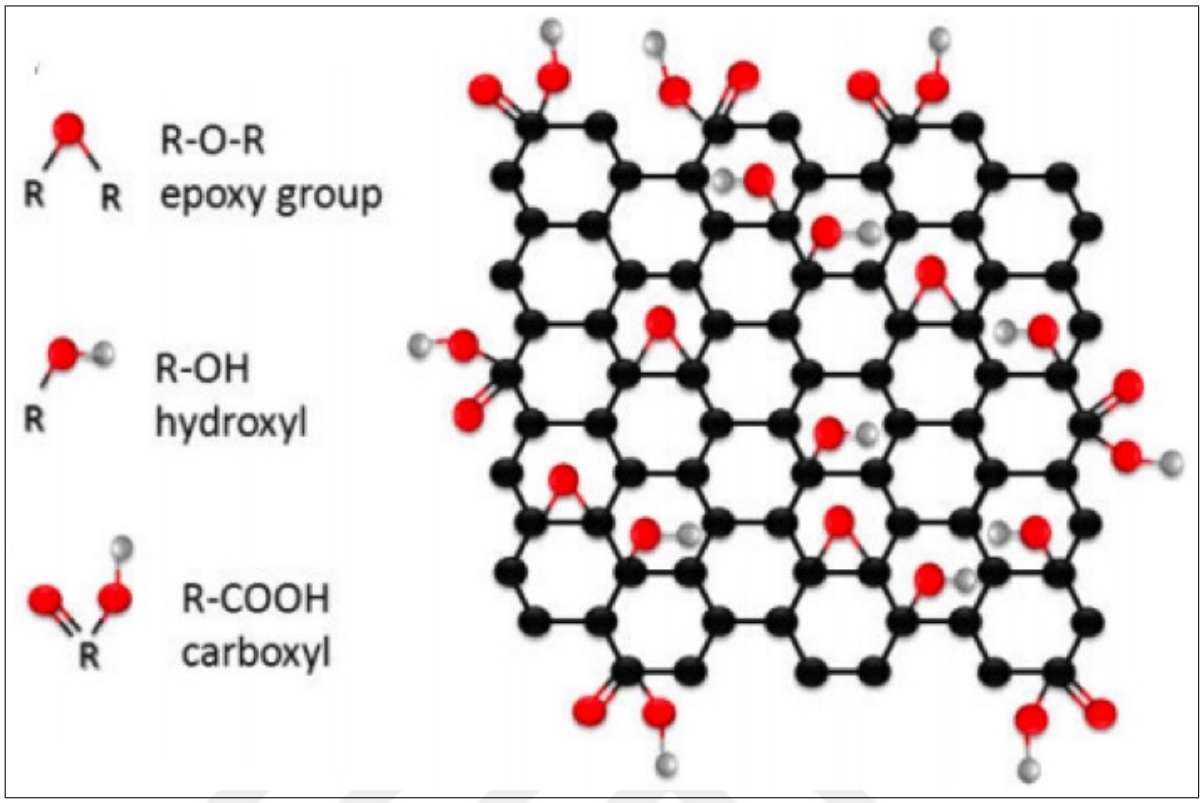

Figure 2.8 The structure of GO and its oxygen containing groups [41]

2.7 Fabrication Techniques of Neural Scaffolds

A number of techniques have been developed to produce neural scaffolds like, particulate leaching [44], extrusion [45], microbraiding [46], gas foaming, freeze-drying [47], phase separation [48], drawing [49], force-spining [50] and electrospinning [6,13,35]. These techniques have fabricated scaffolds with varying degrees of success.

Electrospinning is considered as the most promising technique among them since it offers unique capability for producing nanofibrous scaffolds, similar to native extracellular matrix. Nanofibrous scaffolds also provide several advantages such as a high surface to volume ratio that increase the contact surface area between cells and scaffold, effective mechanical properties, controllable size and shape, tunable porosity and high absorption capacity to design optimal scaffolds for ease of attachment, proliferation and migration of cells [51].

In the electrospinning process, the needle tip and the collector are subjected to high voltage electric field to eject a charged jet of polymer solution from nozzle and carry it to the oppositely charged grounded collector. While the jet moves towards the collector, the solvent evaporates, leading transformation of polymer solution into charged polymer fiber. These charged polymer fibers are laid on the grounded collector to form non-woven nanofibrous mat. The morphology of the nanofibers is mainly based on the solution parameters and process parameters of electrospinning [52]. These parameters are listed below:

I. Solution Parameters

a) Polymeric Solution Concentration

The concentration of polymer solution determines the spinnability of a solution during electrospinning process. There are four critical concentrations of polymer solution from low to high:(1) when the concentration is very low, discrete droplets occur instead of electrospinning due to the low viscosity and high surface tensions of the solution, (2) if the concentration is little higher, beads on fibers are formed, (3) in optimum range of concentration, smooth nanofibers can be fabricated (4) in case of higher concentration, fibers cannot be formed owing to high viscosity. In the optimum range of concentrations, increasing the concentration of solution results in increase in fiber diameter [53, 54].

b) Solvent Composition

Solvent has two essential roles in electrospinning: first is to solubilize the polymer molecules and second is to convey the dissolved polymer molecules to the collector in order to transform them into nanofiber. Therefore, solvent should provide good volatility, vapor pressure and the integrity of the polymer solution during electrospinnig process [55].

c) Conductivity of the Solution

Solution conductivity mainly depends on the polymer and solvent. Suboptimal conductivity of the solution causes inadequate elongation of the

ejected solution to form fine fibers and even may cause beads formation. In the optimal conductivity range, as conductivity of the solution is increased, fiber diameter decreases significantly. However, highly conductive solution results in unstable bending and a broad diameter distribution [54, 55].

d) Solution Viscosity

The polymer solution with low viscosity cannot lead to production of fibers, whereas highly viscous solution leads to difficulties in the ejection from the spinneret. Therefore, optimum solution viscosity should be provided to form smooth fiber. In addition, greater solution viscosity gives rise to increase in the fiber diameter [55, 56].

e) Surface Tension

Surface tension is related to the solvent composition of the solution. Under constant concentration, by lessening the surface tension, smooth fibers can be fabricated [53].

II. Solution Parameters

a) Applied Voltage Applied voltage is a substantial parameter of the electrospinning process. The strength of the applied voltage influences the fiber formation. There is a threshold range for applied voltage to obtain smooth nanofiber. In general, lower or higher applied voltage than the threshold range leads to bead formation [55].

b) Flow Rate Another critical parameter is the flow rate of the solution that effects the nanofiber diameter, porosity and morphology of nanofiber. A low flow rate ensures enough time for the evaporation of solvent and the solidification of nanofibres, whereas too high flow rate leads to formation of beaded fibers due to unavailability of enough drying time prior to reaching the collector. In ideal flow rate range, increasing flow rate results in increase of the diameter and pore size of nanofiber [55, 56].

c) Types of Collectors In the electrospinning process, a collector plays major role as a conductive target to collect nanofibers. There are a variety of collector types with different geometries that can influence fiber morphology

like fiber alignment and pattern. While stationary collectors such as metal plates can be used to generate randomly oriented fibers, parallel electrodes, rotating disks or mandrels can be used to fabricate aligned fibers [55, 57].

d) **Tip to Collector Distance** Although the distance between the tip and the collector does not have significant effect on the nanofiber structure, an optimum distance should be provided to favor solidification of solution before reaching the collector. Otherwise, beads on fibers can be observed [55].

3. MATERIALS AND METHODS

3.1 Fabrication of Electrospun Nanofibers

3.1.1 Fabrication of PLLA Nanofibers

A polymer solution of PLLA was prepared by dissolving PLLA into N,N-Dimethyl Formamide (DMF) at 120°C. Chloroform (Chl) was added and stirred continuously at room temperature until a homogenous solution was obtained. The weight fractions of PLLA were chosen as 6, 7 and 8wt%. For each concentration, the volumetric percentage of DMF in the binary solvent was altered in the range of 0 - 30%.

Then, PLLA solution was electrospun using electrospinning system (NE 300, Inovenso, Turkey) shown schematically in Figure 3.1 The solution was fed into 10 mL syringe with 20 gauge stainless steel blunt needle. The needle tip was placed 15 cm below a rotating mandrel collector and the collector was covered with an aluminum foil. The rotation speed of the mandrel was adjusted to 2064 rpm. The electrospinning process was performed at 1 ml/h flow rate of solution and controlled by a syringe pump. The needle and collector was connected to a high voltage supply and 25kV voltage was utilized to obtain beads free smooth fibers.

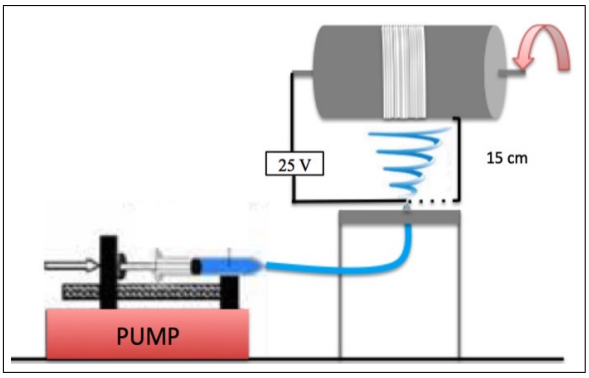

Figure 3.1 Schematic Representation of electrospinnig Process

3.1.2 Fabrication of PLLA/GO Nanofibers

GO solution was diluted with DMF and ultrasonically treated with an ultrasonic homogenization instrument (Bandelin Sonopuls). Sonication was applied for varying times (3, 5, 10 and 15 min) in order to investigate the effect of the sonication time. Then PLLA (7 wt%) was added into the GO/DMF solution and stirred at 120°C. After complete dissolution of PLLA particles, the solution was diluted with chloroform and magnetically stirred at room temperature to obtain a homogenous PLLA/GO solution.

The obtained PLLA/GO solution was electrospun into PLLA/GO nanofibers. The electrospinning process was carried out at a tip to collector distance of 15cm, solution feed rate of 1 ml/h and voltage of 25 kV. The fibers were collected on an aluminum foil which is covering the rotating collector. The rotationspeed of the collector was 2064 rpm.

3.2 Aminolysis of PLLA and PLLA/GO Nanofibers

The polymer nanofiber specimens were cut into a rectangular shape with a dimension of 2x2 cm^2. Then, the specimens were inserted in ethanolic aqueous solution (1:1 v/v) for 3 hours and then they were washed with a large quantity of deionized water and dried. Next, the cleaned specimens were immersed in hexamethylenediamine (HMDA)/ isopropanol (IPA) solution of different concentrations (0.02, 0.04, 0.06 and 0.08 gml^{-1}). For each concentration of the solution varying reaction time intervals (5, 10, 20, and 30 min) was applied at 50°C to determine optimal concentration and reaction time to aminolyze PLLA/GO nanofibers. After this, PLLA fibers were dipped into deionized water for 24 h at room temperature and dried at room temperature [**?**].

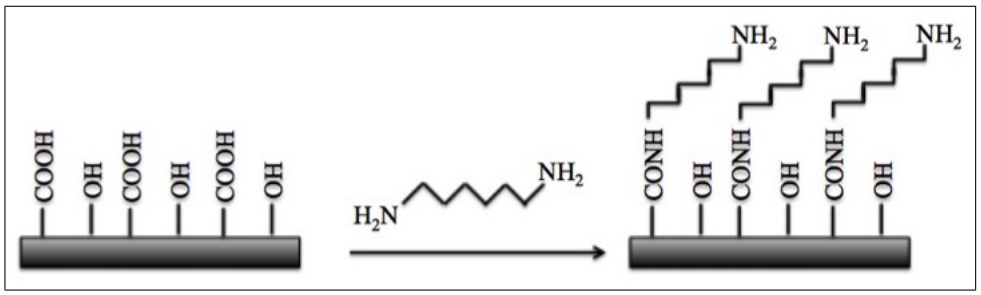

Figure 3.2 Aminolysis reaction of nanofiber surface with HMDA

Cleaned PLLA/GO nanofibers were immersed in 0.04 g/ml HMDA solution for 10 min. After aminolyzation, unreacted HMDA removed by washing samples in deionized water. Then samples were dried at room temperature.

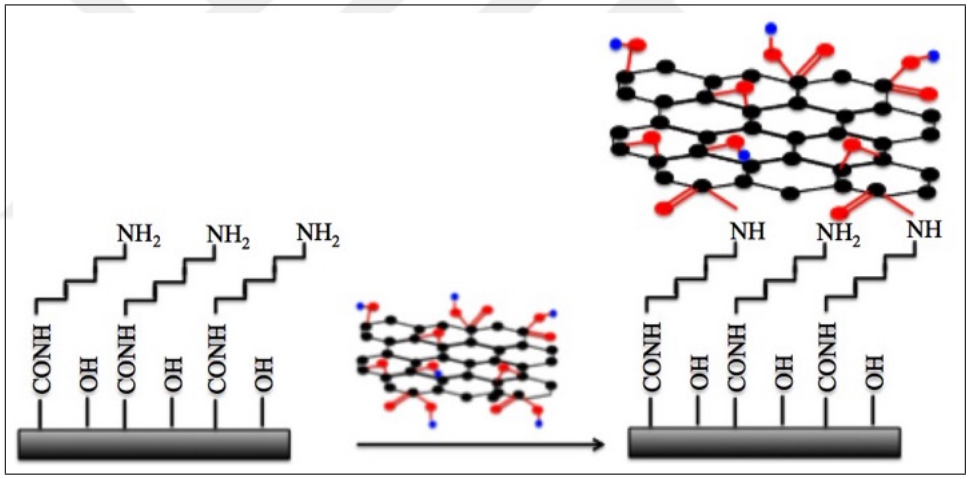

Figure 3.3 Schmeatic representation of GO coated nanofiber

3.3 GO Coating on Aminolyzed PLLA and PLLA/GO Nanofiber

PLLA and PLLA/GO nanofibers were coated with GO by adaptation of method described [?]. GO was dispersed in deionized water by ultrasonication for 10 minutes. GO solution was deposited on the nanofibers for 1 hour and then samples were rinsed gently [12, 58].

3.4 Surface Characterization of PLLA and PLLA/GO Nanofiber

3.4.1 Scanning Electron Microscopy (SEM)

The surface morphology and the orientation of PLLA and PLLA/GO nanofibers were analyzed by using SEM (Philips XL30 ESEM-FEG/ EDAX) at Boğaziçi University Research and Development Center Electron Microscopy and Microanalysis Unit. After coating the specimens with a thin layer of 50 nm gold using a sputter coater, the morphology of the nanofibers was examined with an accelerating voltage of 5 kV. Average diameters of the nanofibers were measured by using SEM images in conjunction with the image analysis software, Image J.

3.4.2 Raman Spectroscopy Analysis

The chemical structure of PLLA and PLLA/GO nanofibers was examined with Raman spectrometer (Renishaw inVia Raman) at Boğaziçi University Advanced Technologies Research and Development Center Raman Microscopy Facility. The excitation wavelength of 532 nm and 50X objective lens was used to obtain a Raman spectrum over the range of 500 cm^{-1} to 3750 cm^{-1}.

3.4.3 Ninhydrin Assay

A ninhydrin assay was used to determine the concentration of NH_2 on the aminoly- zed nanofibers with HMDA. When the ninhydrin reacted with bound amine groups on the surface of nanofibers, a purple compound was formed. This purple compound can be detected with UV-spectrophometer at a maximum wavelength of 538 nm. PLLA and PLLA/GO nanofiber samples were dipped into 1M ninhydrin / ethanol solution for 1 min and then transferred into the glass tubes and heated to 80 C° for 15 min in a water bath. After glass tubes were taken out of the water bath, 2ml of Chl was added to dissolve the nanofiber samples and then 2 ml of IPA was

added to stabilize the color. Absorbance of the final solution was measured at 538 nm with ultraviolet-visible (UV-VIS) spectrophotometer (Thermoscientific Nanodrop 2000). A standard curve that was prepared by known concentration of HMDA solution in Chl/IPA (1:1 v/v) was used to determine the amount of NH_2 deposited on the nanofiber samples [**?**, 59]

3.4.4 X-Ray Photoelectron Spectrophotometer Analysis

Surface elemental composition of GO coated PLLA and PLLA/GO nanofibers was examined using XPS (Thermo Scientific K-alpha X-ray Photoelectron spectrometer) with monochromated aluminum K-alpha X-ray source at 72W, 400 μm spot size, 90° angle and 128 channel detector at Boğaziçi University Advanced Technologies Research and Development Center.

3.4.5 Mechanical Analysis

The mechanical properties of nanofibers were analyzed using a Universal Test Machine (LR 5K Lloyed Instruments, UK) at Boğaziçi University Institute of Biomedical Engineering. The nanofiber specimens were cut into rectangular shapes of 60 x 10 mm^2 in length and width. Thickness of each sample was measured using electronic digital caliper. Ends of each specimen were placed vertically on mechanical gripping part of the tensile tester. Tensile tests were performed at a crosshead speed of 5 mm/min. The measurement was carried out for each nanofiber five times and the mean values were recorded.

3.4.6 Water Contact Angle Measurements

The wettability of the PLLA and PLLA/GO nanofibers was measured with a contact angle measurement device (CAM 101 KSV instruments) at Boğaziçi Univer-

sity Chemistry Department. Approximately 5 μL of deionized water was dropped on the nanofiber surface and images of water on the surface were taken by an integrated camera system and water contact angle was measured and recorded. The measurement was repeated for five different spots of each nanofibers and average value of the measurements was reported.

4. RESULTS

4.1 Optical Microscope Images of PLLA Nanofibers

In the first part of the fabrication of PLLA and PLLA/GO nanofiber scaffolds, the electrospinning parameters were optimized to obtain beads free and fine nanofibers.

PLLA solutions with 6, 7 and 8 wt% concentrations were electrospun under process conditions of 25kV voltage, 1 ml/h flow rate, 2064 rpm speed of the rotating mandrel and 15 cm the tip to the collector distance. Figure 4.1 shows the light microscopy images of PLLA nanofibers.

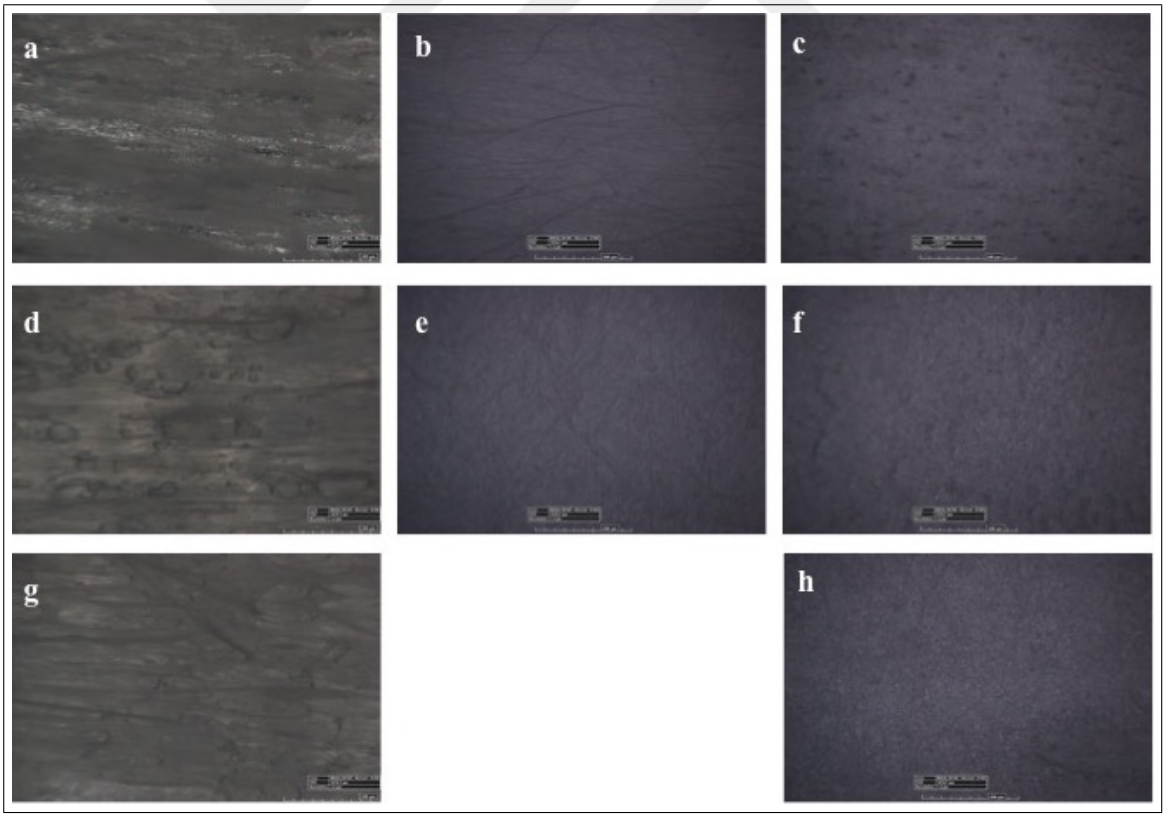

Figure 4.1 Optical Microscope Images of PLLA nanofibers with 6 wt% solution concentration in a.) 0, b.) 20 and c.) 30% DMF, 7wt% solution concentration in c) 0, d.) 20 and e.) 30% DMF and 8wt% g.) 0 and h.) 30% DMF

The microscope images of the nanofibers indicated that there were many beads when the concentration was 6 wt%. However, the nanofibers acquired from PLLA solution with 7 and 8 wt% concentration exhibited beads free and a fine nanofiber structure. Thereafter, 7 and 8 wt% PLLA concentration was investigated further with SEM analysis.

The influence of different volumetric percentages of DMF in binary solvent system on the morphology of nanofibers was examined. It was found that when the percentages of DMF in the solvent were 20 and 30v/v% for 7wt% and 30v/v% for 8 wt% PLLA solution concentrations, beads free fibers could be obtained with the processing parameters of 25 kV, 1 ml/h, 2064 rpm and 15 cm.

4.2 SEM Analysis of PLLA and PLLA/GO Nanofibers

4.2.1 SEM Images of PLLA Nanofibers with Different PLLA Concentrations

The microscopy images showed that 7 wt% PLLA concentration in the solutions containing 20% and 30% DMF and 8 wt% PLLA concentration in the solution with 20% DMF content provided beads free fibers. They were further investigated with SEM as shown in Figure 4.2.

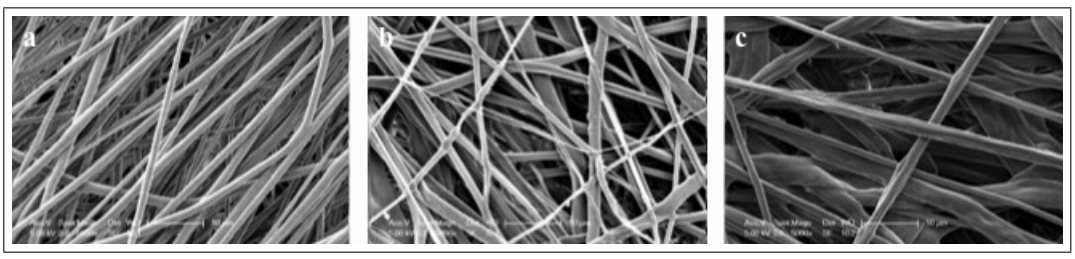

Figure 4.2 7 wt% PLLA in solution containing a.) 20% DMF b.) 30% DMF and c.) 8wt% PLLA in solution with 30 % DMF

The SEM images have shown that, although the nanofibers fabricated from 7 wt% solution concentration with 30% DMF ratio were beads free, they were not uni-

form. 8wt% solution concentration led to uniform, whereas thicker fibers as compared to the fibers obtained from 7 wt% concentration with 20% DMF content. Hence, Chl/DMF ratio of 8/2 for 7wt% led to formation of beads free and thinner PLLA than fibers produced from other concentrations and solvent combinations of Chl and DMF.

4.2.2 SEM Images of PLLA/GO Nanofibers with Different GO Ratio

PLLA/GO nanofibers were fabricated via addition of 0.5, 1, 1.5, 2.5, and 5 v/v% of GO in PLLA solution. SEM images of PLLA/GO were shown in Figure 4.3.

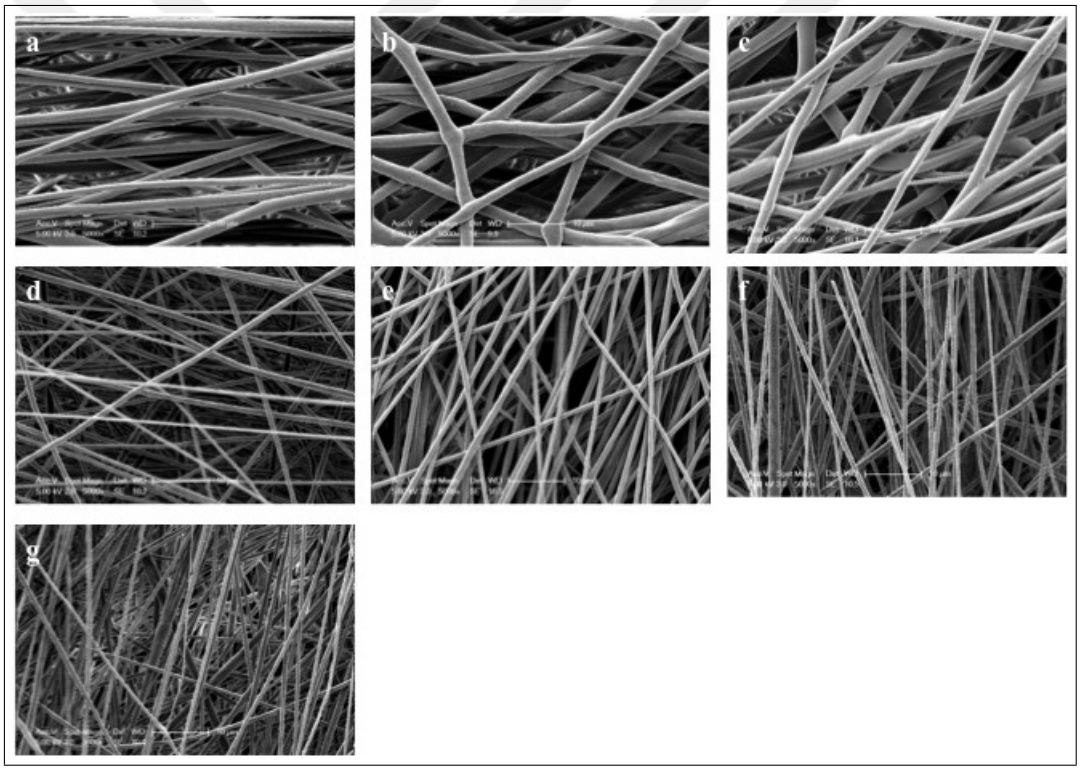

Figure 4.3 PLLA/GO nanofibers with a.) 0.5, b.) 1, c.) 1.5, d.) 2.5, e.) 5, f.) 7.5 and g.) 10% GO ratio

Figure 4.4 shows the average nanofiber diameters of PLLA and PLLA/GO with different GO ratios.

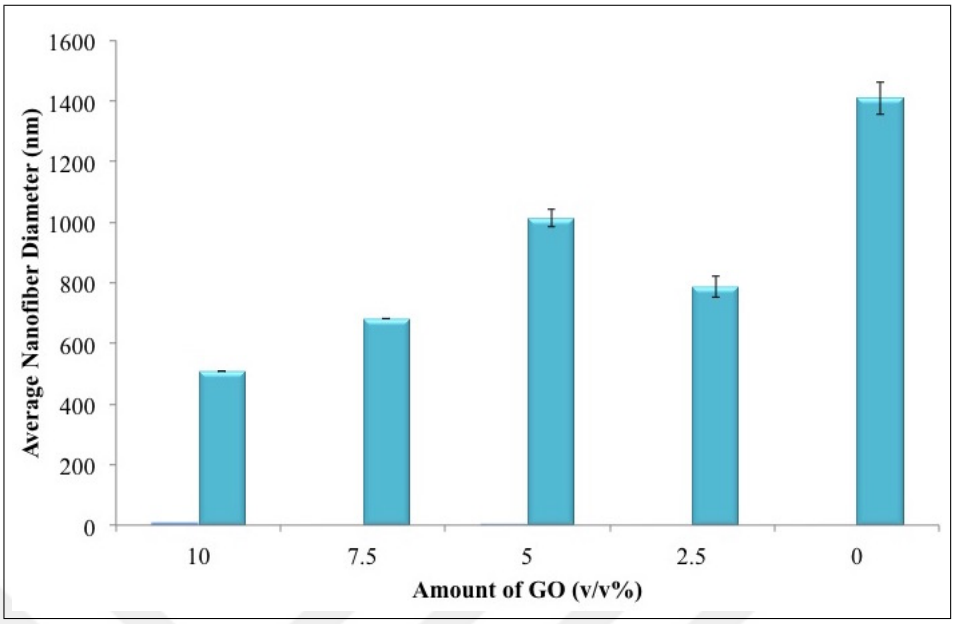

Figure 4.4 Graphical representation of average nanofiber diameter of PLLA and PLLA/GO nanofibers

There was no gradual trend with the increase of wt% of GO but a slight decrease in the average diameter of PLLA/GO nanofiber was observed with the addition 0.5, 1 and 1.5% GO as compared to pure PLLA. The significant decrease in the average nanofiber diameter was observed with the addition of 2.5 and 5% GO and the smallest average nanofiber diameter was obtained from 2.5 v/v% GO. Hereafter, for all other studies 1.5, 2.5 and 5v/v% GO/PLLA were investigated.

4.2.3 SEM Images of Porous PLLA and PLLA/GO Nanofibers

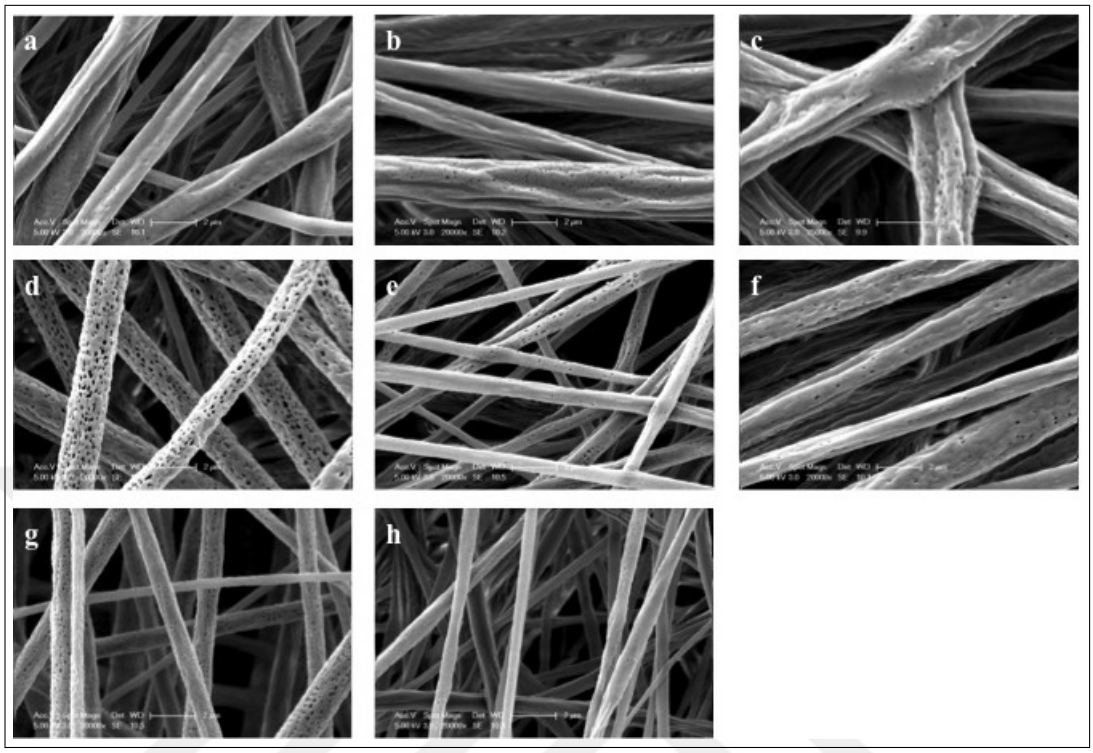

Figure 4.5 Porosity on a.) PLLA and PLLA/GO nanofibers with b.) 0.5 c.) 1 d.) 1.5 e.) 2.5 f.) 5 g.) 7.5 and h.) 10 % GO ratio

SEM images of PLLA and PLLA/GO nanofibers showed that the nanofibers had a porous structure as shown in Figure 4.5, especially PLLA/GO with 1.5% GO exhibited highly porous structure.

4.3 Raman Spectroscopy Analysis of PLLA and PLLA/GO Nanofibers

The chemical structures of the fabricated PLLA and PLLA/GO nanofibers were confirmed by Raman spectroscopy with excitation wavelength of 532 nm.

Raman spectrum of PLLA and GO were shown in Figure 4.6, Figure 4.7 and Figure 4.8.

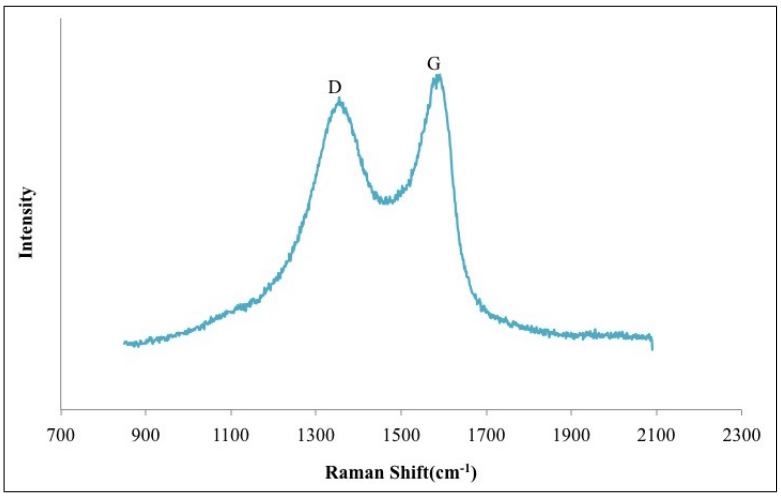

Figure 4.6 Raman spectra of GO sheets

The characteristic peaks of GO were observed at 1379 and 1599 cm^{-1} and they corresponded to the D and G bands respectively. While D bands indicated structural imperfections, G band exhibited sp^2 domain of carbon atoms [12, 13, 43].

The Raman spectrum of pure PLLA was shown in two parts as depicted in Figure 4.7 and Figure 4.8 The recorded raman spectrum in the range of 500 cm^{-1} to 2500 cm^{-1} was shown in Figure 4.7.

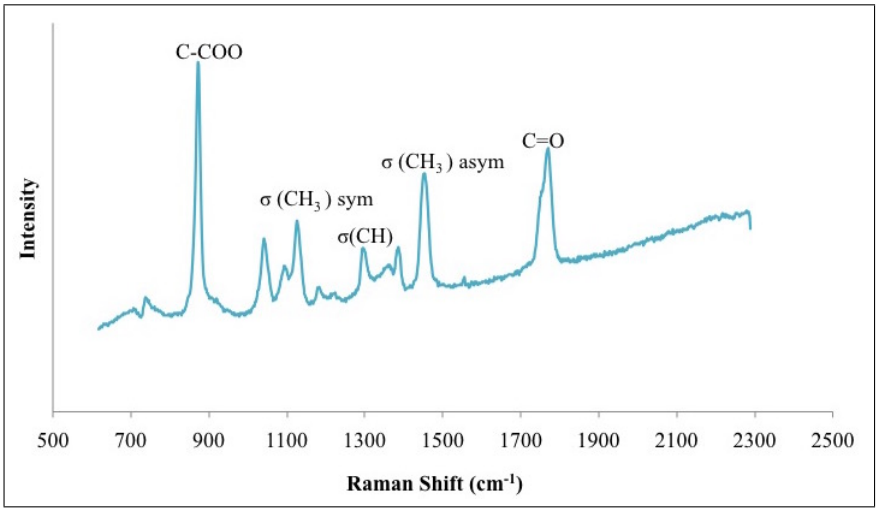

Figure 4.7 Raman spectra of PLLA nanofibers with raman shift between 500-2500 cm^{-1}

The sharp peaks at 873 and 1775 cm^{-1} were attributed to C-COO stretching and C=O stretching, respectively. In addition, the peaks at 1129 cm^{-1}, 1291 cm^{-1}, and 1454 cm^{-1} were assigned to in plane CH_3 bending, CH bending and in plane CH_3 asymmetric bending, respectively.

Raman spectra for PLLA in the range of 2500 - 3750 cm^{-1} was shown in Figure 4.8.

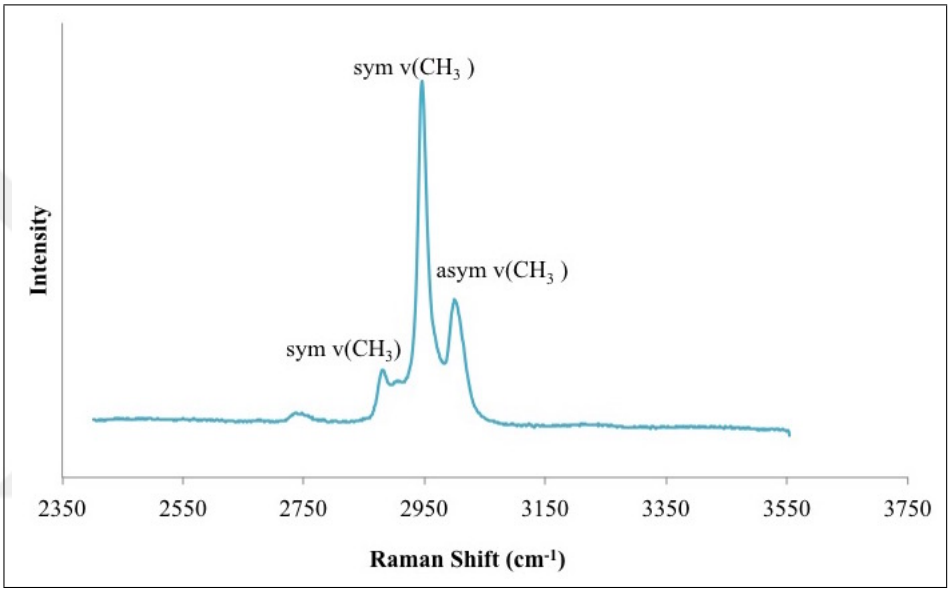

Figure 4.8 Raman spectra of PLLA nanofibers with raman shift between 2400-35500 cm^{-1}

Three prominent peaks were observed at 2885, 2946 cm^{-1} representing symmetric CH_3 stretching and 3004 cm^{-1} indicating asymmetric CH_3 stretching band [60–62]. The Raman spectrum of PLLA, GO and PLLA/GO nanofibers were shown in Figure 4.9.

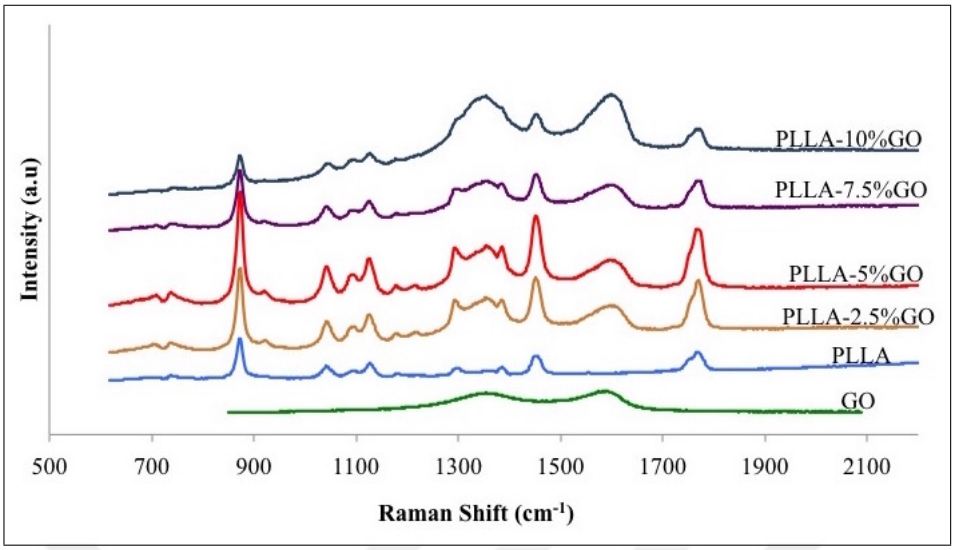

Figure 4.9 Raman Spectra of GO, PLLA and PLLA/GO with different GO ratio

Raman spectras of PLLA/GO nanofibers exhibited characteristic peak of both PLLA and GO. Each spectrum of PLLA/GO nanofibers depicted characteristic PLLA peaks and the shift was observed at 1291 cm^{-1} peak. The composite nanofibers also led to shift in G bands from 1587 cm-1 to 1593, 1597, 1599, 1597 and 1597 cm^{-1} for PLLA/GO nanofibers with 1.5, 2.5, 5, 7.5 and 10% GO, respectively.

Figure 4.10 shows the intensity ratio of D and G bands for PLLA and PLLA/GO nanofibers with different GO ratio.

Intensity ratio of GO was 1.24 and intensity ratios of PLLA/GO nanofibers with 1.5, 2.5, 5, 7.5 and 10% GO ratios were 0.41, 0.67, 0.74, 1.24 and 1.24, respectively. That is, the intensity ratios of PLLA/GO were increased with increasing GO content.

4.4 Ninhydrin Assay

Ninhydrin assay was used to determine quantitatively amount of NH_2 on aminolyzed PLLA surface with HMDA. The purple compound produced from reaction between ninhydrin and free NH_2 has a maximum absorbance at 538 nm [**?**, 59].

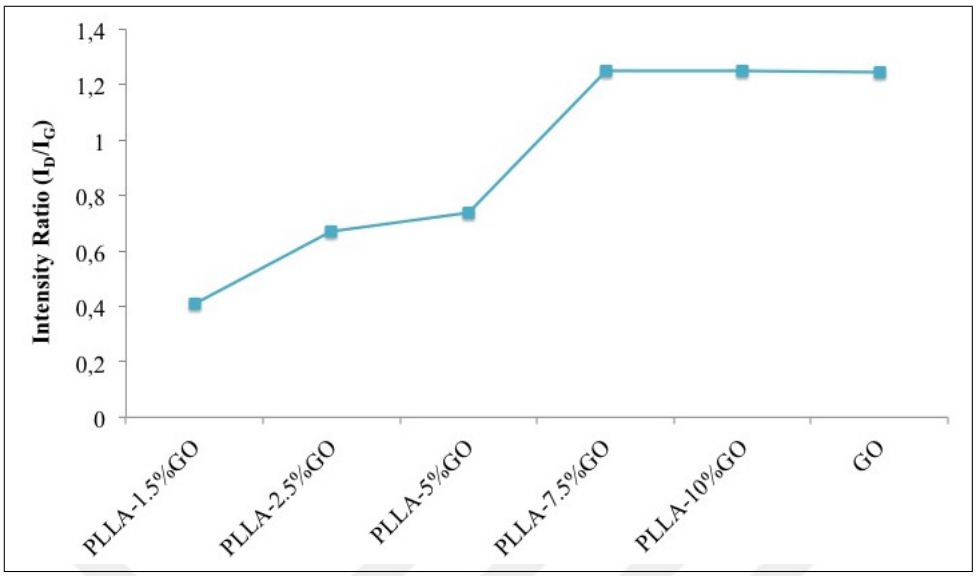

Figure 4.10 Intensity ratio of PLLA and PLLA/GO nanofibers

According to standard curve, amount of NH_2 on the surface of nanofibers were calculated by using measured absorbance of dissolved nanofibers in Chl/IPA solution and demonstrated in Figure 4.11.

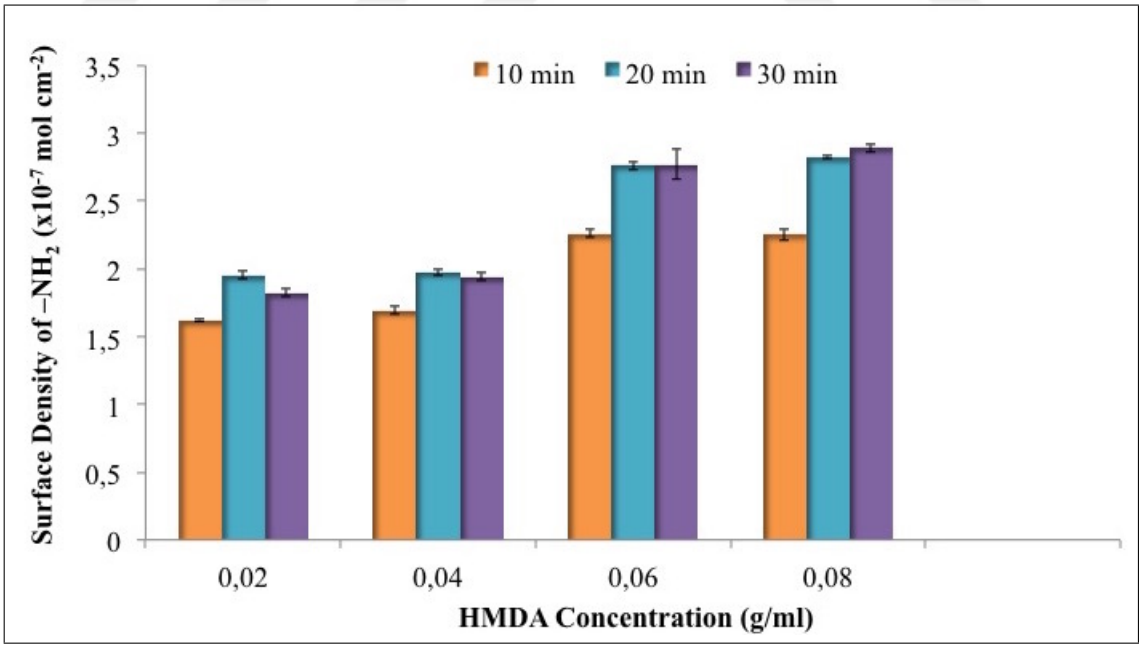

Figure 4.11 Surface density of NH_2 versus HMDA concentration graph

4.5 XPS Analysis of GO Coated PLLA and PLLA/GO Nanofibers

Surface chemical compositions of GO coated PLLA and PLLA/GO nanofibers were examined using XPS analysis techniques. Figure 4.12 depicted XPS survey spectrum of GO coated PLLA/GO nanofiber with 1%GO ratio.

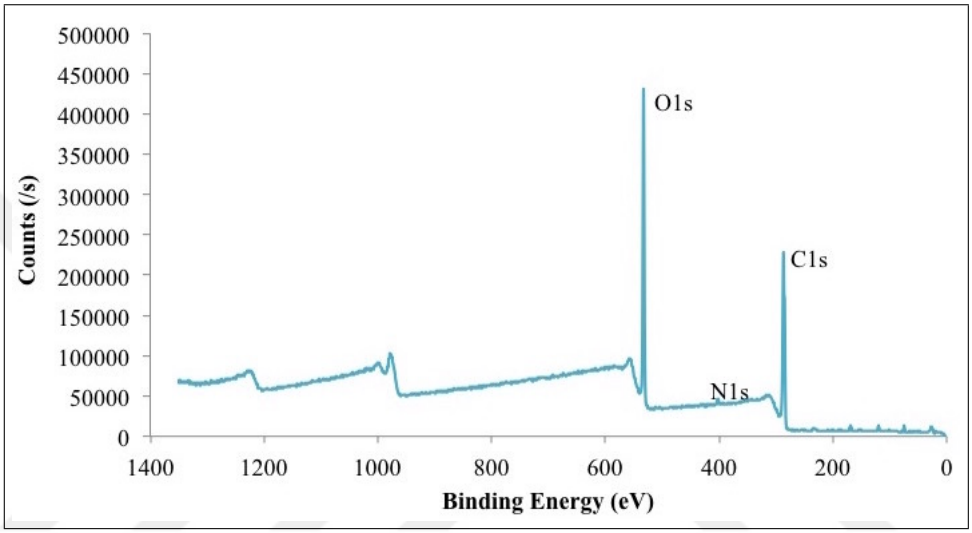

Figure 4.12 Survey spectrum of PLLA/GO nanofiber with 1.5% GO ratio

The survey spectrum demonstrated three sharp peaks at 533, 400 and 287 eV representing N1s, O1s and C1s respectively. C1s, N1s and O1s core levels were deconvoluted to obtain detailed information about chemical bonds between elements.

In Figure 4.13, the high-resolution C1s peak of GO coated PLLA/GO nanofiber with 1%GO concentration was deconvoluted into five different peaks.

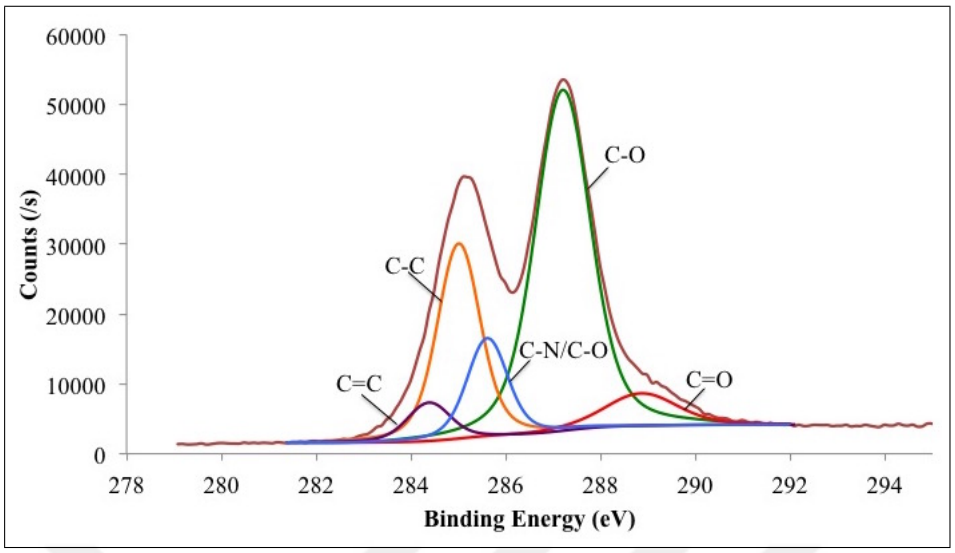

Figure 4.13 High-resolution spectra of C1s of PLLA/GO nanofiber

The prominent peaks on the had binding energies of 288.86, 287.2, 285.61, 285, and 284.28 eV corresponding to O=C-OH (carboxyl group), C=O (carbonyl group), C-N/C-O (hydroxyl and epoxy) [63] , C-C and C=C (aromatic hydrocarbon) [64], [65].

In Figure 4.14, high-resolution spectra of N1s showed different peaks of nitrogen.

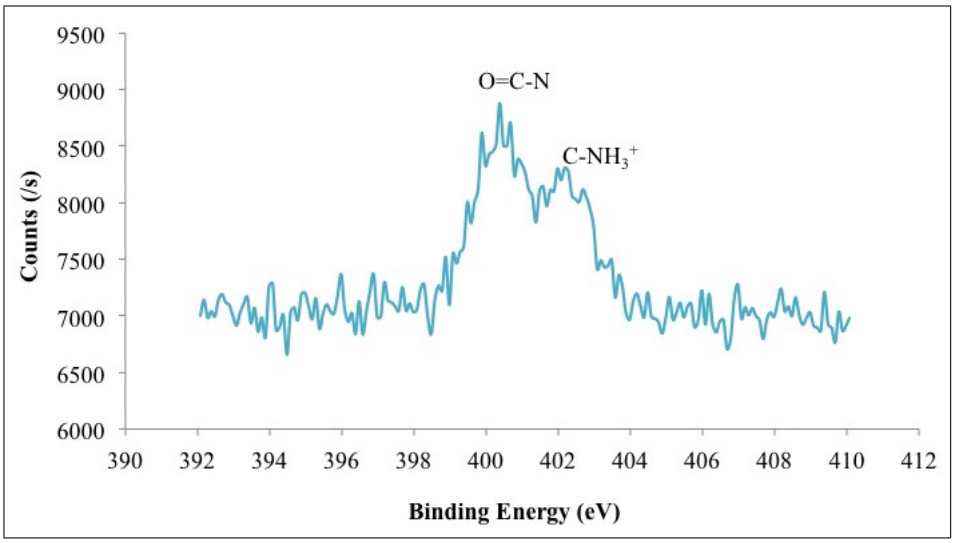

Figure 4.14 High-resolution spectra of C1s of PLLA/GO nanofiber

The peaks at 402.28 and 400 eV binding energies were attributed to free amine

group (C-NH_3+) and amide bond (O=C-N) [66].

4.6 Mechanic Analysis of PLLA and PLLA/GO Nanofibers

The mechanical properties of PLLA and PLLA/GO nanofibers were investigated using tensile test. The stress-strain curve of PLLA and PLLA/GO nanofibers were shown in Figure 4.15.

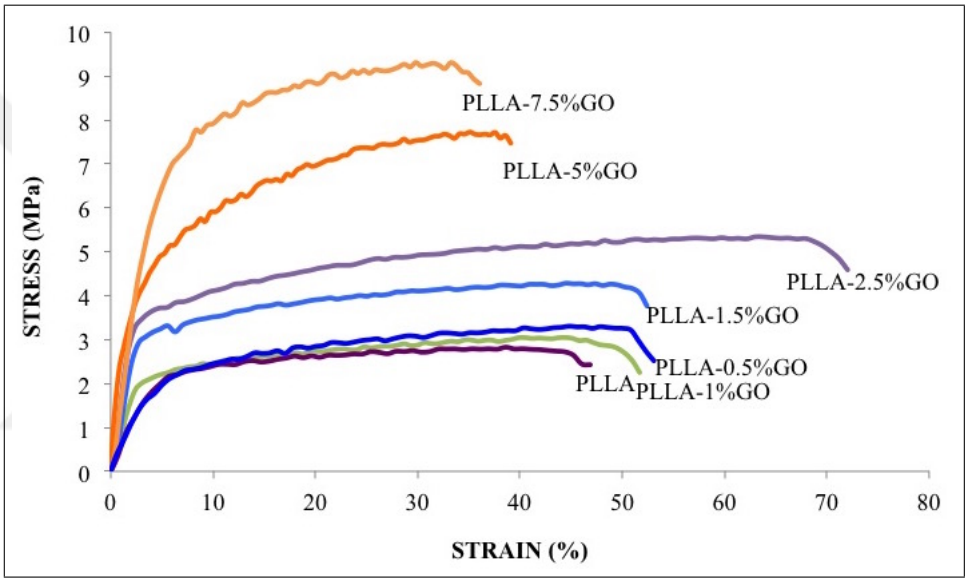

Figure 4.15 Stress- strain curve of PLLA and PLLA/GO nanofibers

The graph showed that increasing GO ratio in PLLA/GO composite nanofibers increases the strength of the structure and yields significant improvement in strength was observed with addition 7.5v/v%GO ratio.

The ultimate tensile strength (UTS) graph of the nanofibers was reported in Figure 4.16.

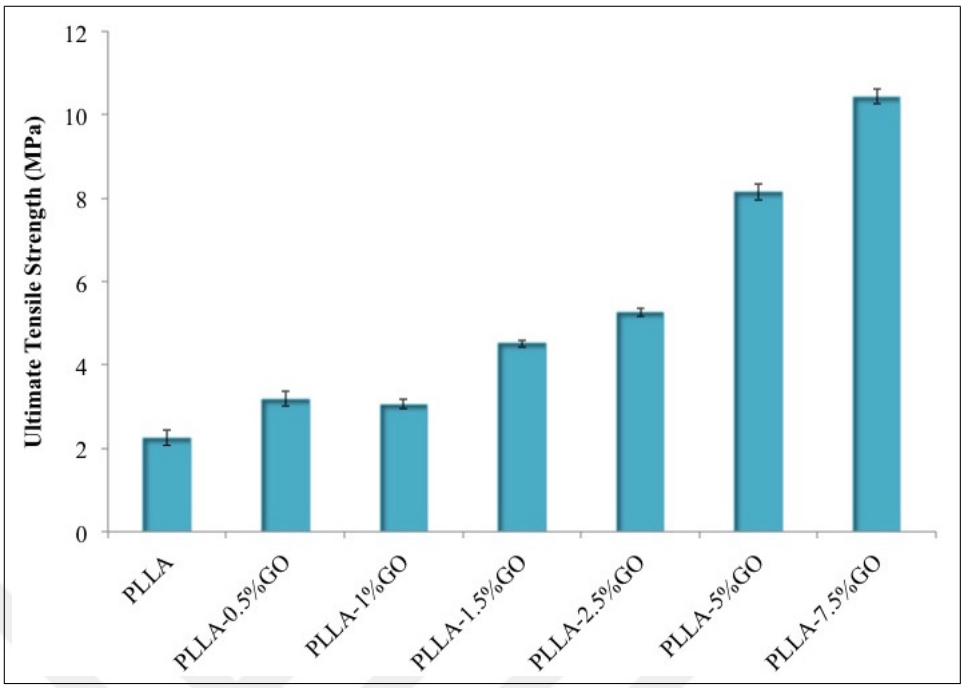

Figure 4.16 Ultimate tensile strength graph of PLLA and PLLA/GO nanofibers

As seen in the graph, while pure PLLA had 2.249 ± 0.902 MPa UTS, PLLA/GO nanofibers with 0.5, 1, 1.5, 2.5, 5 and 7.5% GO ratio showed 3.188 ± 0.866, 3.055 ± 0.586, 4.508 ± 0.471, 5.262 ± 0.494, 8.136 ± 0.956 and 10.435 ± 0.881 MPa. Namely, the tensile strength of the nanofibers enhanced gradually with increasing GO ratio.

The obtained data from the stress-strain curve were used to calculate Young's Modulus of PLLA and PLLA/GO nanofibers and they were tabulated in the graph as depicted in Figure 4.17.

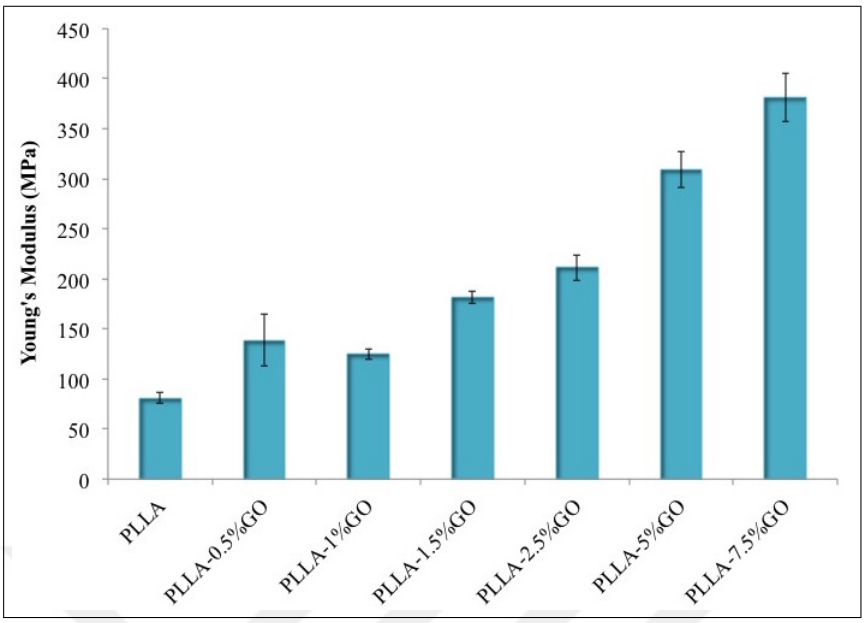

Figure 4.17 Young's Modulus of PLLA and PLLA/GO nanofibers

The Young's Modulus values of PLLA and PLLA/GO nanofibers with 0.5, 1, 1.5, 2.5, 5 and 10%GO ratios were calculated as 66.47 ± 24.51, 97.30 ± 68.27, 97.52 ± 11.72, 151.42 ± 18.61, 176.67 ± 47.64, 230.19 ± 31.18 and 318.22 ± 92.25 MPa. This means that the Young's Modulus values increased with increasing GO ratio in the composite nanofibers.

The graph of percentage elongation at break values for PLLA and PLLA/GO nanofibers was plotted in Figure 4.18.

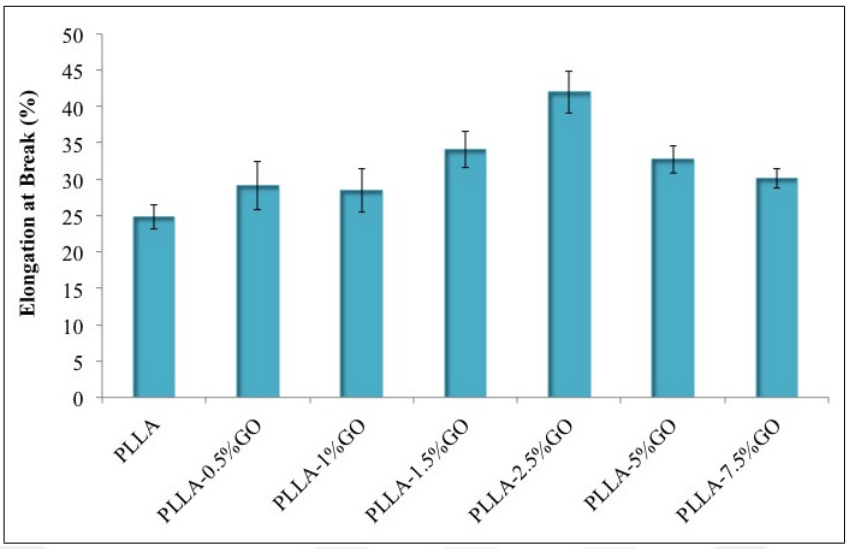

Figure 4.18 Percentage elongation at break graph of PLLA and PLLA/GO Nanofibers

The average values of elongation at break for PLLA/GO nanofibers with 0.5, 1, and 7.5% GO ratio slightly changed from the elongation at break value of PLLA (24.78 %). However, the average elongation at break values of PLLA/GO nanofibers with 1.5 and 2.5% GO increased to 34.05 and 42 % respectively.

4.7 Water Contact Angle Measurements

4.7.1 Water Contact Angle Analysis of PLLA and PLLA/GO Nanofibers

The water contact angles of PLLA and PLLA/GO nanofibers were measured to investigate the effect of addition of GO as filler on wettability of PLLA and PLLA/GO nanofibers. The captured images of a drop of water on the surface of nanofibers at 3rd second were shown in Figure 4.19.

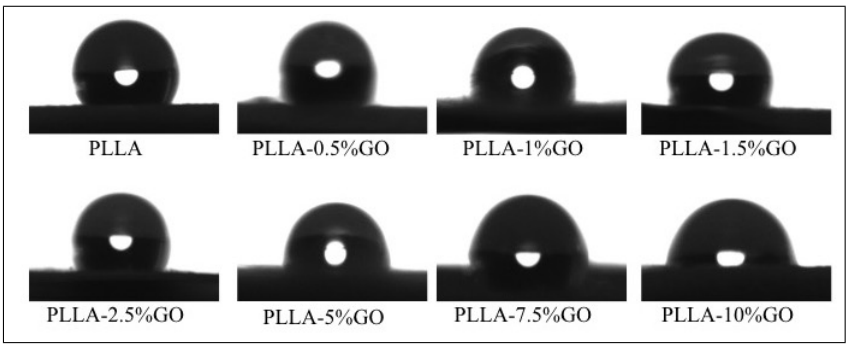

Figure 4.19 Water contact angle images of PLLA and PLLA/GO Nanofibers

The water contact angle values of PLLA and PLLA/GO nanofibers with different GO ratio were shown in Figure 4.20.

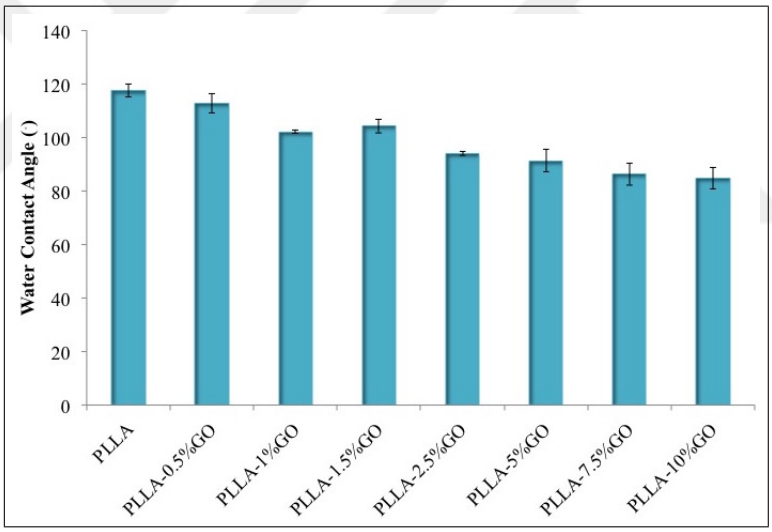

Figure 4.20 Water contact angle graph of PLLA and PLLA nanofibers

The average contact angle values of the water drops on the PLLA and PLLA/GO nanofibers with 0.5, 1, 1.5, 2.5, 5, 7.5 and 10%were 117.5°, 112.6°, 102°, 104.2°, 94.1°, 91.3, 86.3 and 84.7 respectively. The results indicated that the addition of GO increased the hydrophilicity of PLLA/GO composite nanofibers as compared to pure PLLA.

4.7.2 Water Contact Analysis of GO coated PLLA and PLLA/GO Nanofibers

The effect of surface coating of PLLA and PLLA/GO nanofibers with GO on wettability of the nanofibers were analyzed with water contact angle measurements and capture images at 3rd second were shown in Figure 4.21.

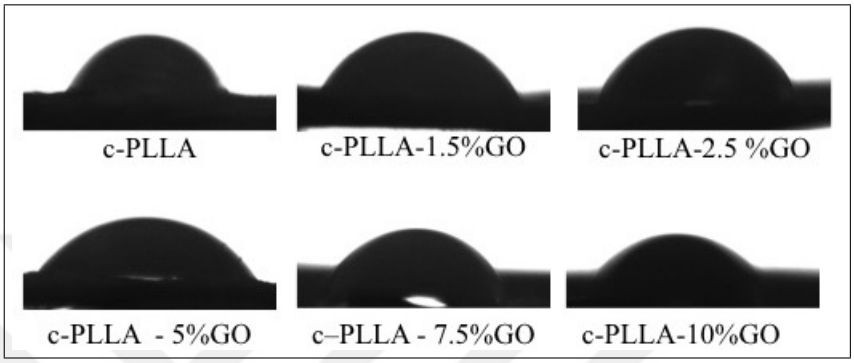

Figure 4.21 Water contact angle images of GO coated PLLA and PLLA/GO nanofibers

The contact angle values of PLLA and PLLA/GO nanofibers with 1.5, 2.5, 5, 7.5 and 10% GO were 76.5°, 71.9°, 61.2°, 57.8°, 49.9° and 48.5° respectively.

5. DISCUSSION

Peripheral nerve injury is a prevalent health problem and generally leads to serious consequences such as life-long disability [31]. Although many techniques have been exploited for nerve regeneration and repair, even the gold standard technique, namely, autologous nerve grafts are not sufficient for its treatment. Therefore, many researches have been conducted to develop alternative treatment strategies for peripheral nerve injuries. Tissue engineered nerve grafts have been considered as a potential treatment strategy [1].

PLLA has been used as a biodegradable and biocompatible synthetic polymer with good mechanical integrity to fabricate nanofibrous scaffolds for nerve tissue engineering applications. However, the research results showed that PLLA alone is not a suitable biomaterial for the fabrication of scaffold due to lack of binding sites for cellular interactions. Hence, to enhance bioactivity, biocompatibility and physical properties, PLLA is incorporated with bioactive materials [67, 68]. Graphene oxide is considered as a novel supplementary material thanks to its surface chemistry, high mechanical properties, conductivity and wettability [11]. Many researches have shown that incorporation of GO to synthetic materials enhanced the cellular interaction, growth and differentiation of a wide range of cell lines [12,13]. Based on these results, incorporation of GO in the scaffolds matrix leads to remarkable improvement in the properties of the scaffolds.

In this thesis, GO was incorporated into PLLA matrix as a filler, coating material and both filler and coating material to investigate effect of GO on the physical, chemical and mechanical properties of electrospun nanofiber scaffolds.

5.1 Morphological Properties of PLLA And PLLA/GO Nanofibers

In the first part of the study, in order to obtain beads free, uniform and a thin fiber in nano range, the solution parameters of electrospinning process were optimized. 6, 7 and 8 wt% PLLA solution was prepared in DMF and Chl binary solvent. 0, 20 and 30 v/v % DMF were used in the solvent in order to investigate the ideal concentration for the electrospinning of PLLA nanofibers. Morphological properties of nanofibers were analyzed using optical microscope and SEM. The images showed that although beads were observed widely on the nanofibers fabricated from PLLA solution with 6wt % concentration, the nanofibers fabricated with 7 and 8 wt% concentration exhibited beads free nanofibers. At a low concentration, the solution could not dry before reaching the collector and this wet polymer fibers dried due to surface tension and the relaxation process. On the other hand, fibers dried before reaching the collector at higher concentration [69]. In addition, when the average nanofiber diameter was analyzed, nanofibers fabricated from 8wt% concentration with 30% DMF in the solvent phase had a greater average nanofiber diameter as compared to nanofibers fabricated from 7wt% PLLA in the solution with 30% DMF content. For the reason that, a higher concentration of PLLA had a higher viscosity which led to resistance to jet elongation and thinning, which ultimately caused formation of a thicker fiber diameter [70]. Electrospining PLLA solution with solely Chl solvent led to formation of a film instead of a nanofiber. With the addition of 20 and 30% DMF, nanofibers could be obtained for 7 wt% PLLA. Additionally, nanofibers could also be obtained for 8 wt% PLLA with 30% DMF. Since, chloroform is a highly volatile solvent, it evaporated immediately when used alone. However, the addition of DMF in the solvent led to decrease in the volatility of the solution and solvent evaporated completely just before reaching the collector [71].

The average nanofiber size decreased with the addition of GO from 2566 nm to 787 nm since GO is a conductive material and with increasing the GO ratio conductivity of the solution increased, so a highly conductive solution carried more charge, which led

to a stronger tensile force to applied voltage. This facilitated to formation of thinner fibers [72].

5.2 Chemical Analysis of PLLA And PLLA/GO Nanofibers

In this thesis, PLLA was reinforced with different weight fractions of GO to improve physical and chemical properties of PLLA matrix. The integration of GO in PLLA as filler was analyzed with the Raman spectroscopy. While Raman analysis of GO showed characteristic D and G bands at 1379 cm^{-1} and 1587 cm^{-1} respectively, the Raman spectra of PLLA exhibited the prominent peaks at 873 cm^{-1}, 1454 cm^{-1} and 1775 cm^{-1} assigned to C-COO stretching, in plane CH_3 asymmetric bending and C=O respectively. The Raman analysis of PLLA/GO composite nanofibers showed both characteristics peaks of GO and PLLA. Additionally, the shifts were observed at G band of GO from 1587 cm^{-1} for GO to 1597 cm^{-1} for PLLA/GO nanofibers [14, 73]. These all proved that GO dispersed in PLLA matrix [73]. Intensity ratio of D and G bands for PLLA/GO nanofibers increased with increasing wt% of GO in the composite nanofiber. It can be deduced that by the incorporation of GO with a higher ratio in the PLLA matrix, the number of defects on GO structure decreased, which confirmed interaction of GO with PLLA [74].

After preparation of PLLA and PLLA/GO nanofibers, the surface of PLLA and PLLA/GO was functionalized with HMDA. The degree of functionalization of PLLA with HMDA was characterized with ninhydrin assay. Different reaction times (10, 20 and 30 minutes) and HMDA concentrations (0.02, 0.04, 0.06 and 0.08 g/ml) were used and the results showed that increasing reaction time and concentration both increased the surface density of NH_2 from 1.62 x 10^{-7} mol/cm2 to 2.89 x 10^{-7} mol/cm^2. However, a reaction time longer than 10 minutes and a concentration higher than 0.04 g/ml caused loss in the mechanical integrity of nanofibers because aminolysis reaction condition become severe and affected mechanical properties of the nanofibers. These results were compatible with previous studies [**?**, 75]. Therefore, PLLA and PLLA/GO were aminolyzed with 0.04 g/ml HMDA concentration for 10 minutes to

ensure mechanical properties during aminolyzation of the nanofibers.

Surface topography and chemical properties has important effects on cellular interactions. Hence, PLLA and PLLA/GO nanofibers were coated with GO to improve the biocompatibility and bioactivity of their surfaces. GO sheets were coated on the aminolyzed PLLA and PLLA/GO nanofibers through a reaction between amine groups on the surface and carboxyl groups on GO sheets [76]. Surface treatments on PLLA and PLLA/GO with GO were confirmed by XPS analysis. The survey spectrum of the coated PLLA and PLLA/GO nanofibers showed the N1s, O1s and C1s peaks. The high resolution XPS spectrum of C1s regions had five peaks at binding energies of 284.28, 285.01, 285.61, 287.2 and 288.86 eV attributed to C=C, C-C, C-N/C-O, C=O and O=C-OH bonds in the GO, respectively [63–66]. The presence of O=C-OH peaks confirmed the coating of PLLA/GO nanofiber with GO. High resolution XPS spectrum of N1s showed two prominent peaks at 400 and 402.28 eV assigned to amide bond and free amine group. The amide peak at the N1s spectrum region and C-N peak at C1s spectrum region proved the functionalization nanofibers with HMDA [4, 63].

5.3 Mechanical Analysis of PLLA and PLLA/GO Nanofibers

Tissue engineered scaffolds for nerve regeneration should mimic the biomechanical properties of peripheral nerve to support a three dimensional structure and cellular interactions. The peripheral nerves in situ are mainly exposed to tensile stress with shear and compressive stress [24]. Therefore, in this study the tensile stress, the elongation at break and Young's Modulus of the fabricated nanofiber scaffolds were investigated to design appropriate scaffold for potential peripheral nerve regeneration application. The ultimate tensile strength of PLLA and PLLA/GO were measured and it was seen that average tensile strength of the nanofibers increased gradually from 3.188 MPa to 10.435 MPa with the addition of 7.5 wt% GO in pure PLLA. The obtained results were close with the biomechanical values of peripheral nerve whose average tensile strength was 11.7 MPa [24]. The Young's Modulus values were calculated by using stress-strain curve and the results of average Young's Modulus values

increased from 66.47 MPa to 318.22 MPa with the addition of GO. Enhancement in the mechanical properties of the nanofiber with addition of GO was provided by well dispersion of GO in the PLLA matrix leading to transfer stress from PLLA matrix to GO sheets [77,78]. The elongation at break values of the nanofibers were measured and although there were no obvious trend, the elongation at break values were increased for PLLA/GO nanofibers with GO ratio up to 2.5%. However higher GO ratio in the nanofibers led to decrease in the elongation at break values. Main reason for this was probably agglomeration of GO sheets in the nanofibers [**?**].

5.4 Wettability of PLLA and PLLA/GO Nanofibers

The surface wettability of the electrospun nanofibers has a significant role for cellular interaction. Namely, hydrophilic scaffolds favor the attachment, proliferation and migration of the cells. In this thesis, the water contact angle PLLA, PLLA/GO and coated PLLA and PLLA/GO nanofibers were measured to analyze the surface wettability of the nanofibers. Before incorporation of GO, the average contact angle of PLLA was measured as 117.5°. The average contact value of the nanofibers decreased to up to 84.7 with the addition of 10 wt% GO. Hereby, the partial interaction of oxygen containing groups in GO and water increased the wettability of nanofibers with increasing GO ratio [**?**]. For further improvement, the surface of PLLA and PLLA/GO nanofibers were coated with GO and the water contact angle of the samples were measured. The results showed that surface treatment further increased the wettability of nanofiber surfaces thanks to direct interaction between oxygen containing groups of GO and water. The wettability results of PLLA, PLLA/GO and GO coated PLLA and PLLA/GO nanofibers were in good agreement with the previous work [13, 79].

6. CONCLUSIONS

6.1 Conclusions

This study involves the combination of the chemical, physical and mechanical properties of GO with morphological structure of PLLA nanofibers to develop electrospun PLLA/GO scaffolds in an effort to produce potential scaffolds for regeneration of injured peripheral nerves. The optical microscopy and SEM images have shown that fibers without any beads were fabricated from 7wt% PLLA solution in Chl/DMF solvent with 20%DMF composition. Increasing GO ratio decreased the average nanofiber diameter from 1407 to 507nm. Moreover, SEM images have shown that PLLA and PLLA/GO nanofibers had porous structure and addition of GO increased the porosity of the nanofibers.

The surface of PLLA and PLLA/GO nanofibers were coated with GO via linker molecule of HMDA. The surface density of NH_2 on the nanofibers was measured by ninhydrin assay and the results demonstrated that the ideal aminolyzation reaction was carried out with 0.04 g/ml HMDA concentration at 50C° for 10 minutes and the amount of NH_2 was measured as 1.69 x 10^{-7} mol/cm^2. The functionalization of nanofibers with HMDA and the integration of GO into and onto PLLA were confirmed by Raman and XPS analyses.

The existence of GO also enhanced the mechanical properties of nanofibers. The ultimate tensile strength and Young's Modulus of nanofibers were increased by 364% and 379% respectively. However, the elongation at break values exhibited little improvement. Afterwards, the wettability of the nanofibers was examined by WCA. The results indicated that addition of GO into the PLLA nanofibers increased the average contact angle of water droplet on the nanofibers from 117.5° to 84.7° and wettability of the nanofiber surfaces were further improved by the coating surface of nanofibers with GO. The average contact angle decreased to 48.5° after coating

PLLA/GO nanofiber with 10% GO ratio with GO.

In conclusion, PLLA and PLLA/GO nanofibers were prepared and characterized through SEM, Raman spectroscopy, XPS, tensile test and water contact angle measurements. The results confirmed that the addition of GO enhanced chemical, physical and mechanical properties of the nanofibers. To improve the surface chemical properties further, the nanofibers were coated with GO and results proved that GO coated nanofibers led to increase in the wettability.

6.2 Future Studies

In this study, the results revealed that the addition of GO led to enhanced chemical and physical properties of fibers which is promising for nerve regeneration applications. As a future work, the porosity level of the nanofibers depending on the concentration and sonication time of GO will be examined. Finally, the effect of porosity, chemical, physical and mechanical properties of PLLA, PLLA/GO and GO coated PLLA and PLLA/GO nanibers on Schwann cell response will be assessed.

APPENDIX A. CALIBRATION CURVE

The standard curve obtained from known concentration of HMDA in Chl /IPA solution (1:1 v/v) was plotted as shown in Figure A.1.

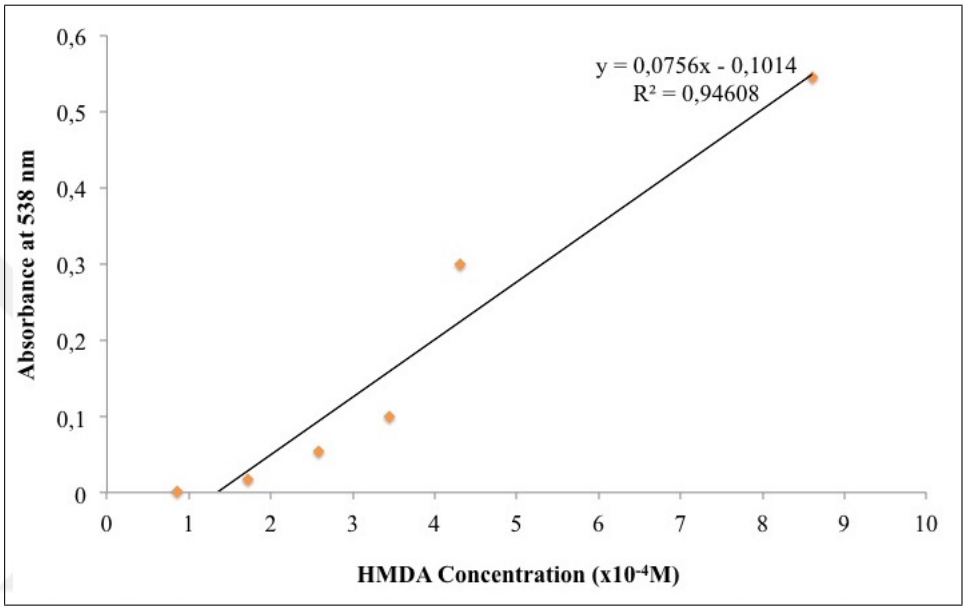

Figure A.1 Water contact angle images of GO coated PLLA and PLLA/GO nanofibers

REFERENCES

1. Gu, X., F. Ding, and D. F. Williams, "Neural tissue engineering options for peripheral nerve regeneration," *Biomaterials*, Vol. 35, no. 24, pp. 6143–6156, 2014.

2. Gutierrez, A., and J. D. England, *Peripheral Nerve Injury*, pp. 863–869. New York, NY: Springer New York, 2014.

3. Daly, W., L. Yao, D. Zeugolis, a. Windebank, and a. Pandit, "A biomaterials approach to peripheral nerve regeneration: bridging the peripheral nerve gap and enhancing functional recovery," *Journal of The Royal Society Interface*, Vol. 9, no. 67, pp. 202–221, 2012.

4. Subramanian, A., U. M. Krishnan, and S. Sethuraman, "Development of biomaterial scaffold for nerve tissue engineering: Biomaterial mediated neural regeneration.," *Journal of biomedical science*, Vol. 16, p. 108, 2009.

5. Johnson, E. O., and P. N. Soucacos, "Nerve repair: Experimental and clinical evaluation of biodegradable artificial nerve guides," *Injury*, Vol. 39, no. 3 SUPPL., pp. 29–33, 2008.

6. Hu, A., B. Zuo, F. Zhang, Q. Lan, and H. Zhang, "Electrospun silk fibroin nanofibers promote Schwann cell adhesion, growth and proliferation," *Neural Regeneration Research*, Vol. 7, pp. 1171–1178, may 2012.

7. Zamani, F., M. Amani-Tehran, M. Latifi, and M. A. Shokrgozar, "The influence of surface nanoroughness of electrospun PLGA nanofibrous scaffold on nerve cell adhesion and proliferation," *Journal of Materials Science: Materials in Medicine*, Vol. 24, no. 6, pp. 1551–1560, 2013.

8. Asran, A., M. Salama, C. Popescu, and G. Michler, "Solvent Influences the Morphology and Mechanical Properties of Electrospun Poly(L-lactic acid) Scaffold for Tissue Engineering Applications," *Macromolecular Symposia*, Vol. 294, no. 1, pp. 153–161, 2010.

9. Rasal, R. M., A. V. Janorkar, and D. E. Hirt, "Poly(lactic acid) modifications," *Progress in Polymer Science (Oxford)*, Vol. 35, no. 3, pp. 338–356, 2010.

10. Ahadian, S., M. Ramalingam, and A. Khademhosseini, "The Emerging Applications of Graphene Oxide and Graphene in," *Biomimetics*, pp. 279–300, 2013.

11. Jin, L., D. Yue, Z.-W. Xu, G. Liang, Y. Zhang, J.-F. Zhang, X. Zhang, and Z. Wang, "Fabrication, mechanical properties, and biocompatibility of reduced graphene oxide-reinforced nanofiber mats," *RSC Advances*, Vol. 4, p. 35035, 2014.

12. Shah, S., P. T. Yin, T. M. Uehara, S.-T. D. Chueng, L. Yang, and K.-B. Lee, "Guiding Stem Cell Differentiation into Oligodendrocytes Using Graphene-Nanofiber Hybrid Scaffolds," *Advanced Materials*, Vol. 26, no. 22, pp. 3673–3680, 2014.

13. Chaudhuri, B., D. Bhadra, L. Moroni, and K. Pramanik, "Myoblast differentiation of human mesenchymal stem cells on graphene oxide and electrospun graphene oxide olymer composite fibrous meshes: importance of graphene oxide conductivity and dielectric constant on their biocompatibility," *Biofabrication*, Vol. 7, no. 1, p. 015009, 2015.

14. Zhang, C., L. Wang, T. Zhai, X. Wang, Y. Dan, and L. S. Turng, "The surface grafting of graphene oxide with poly(ethylene glycol) as a reinforcement for poly(lactic acid) nanocomposite scaffolds for potential tissue engineering applications," *Journal of the Mechanical Behavior of Biomedical Materials*, Vol. 53, pp. 403–413, 2016.

15. Heath, C. A., and G. E. Rutkowski, "The development of bioartificial nerve grafts for peripheral-nerve regeneration," *Trends in Biotechnology*, Vol. 16, no. 4, pp. 163–168, 1998.

16. Ide, C., "Peripheral nerve regeneration," 1996.

17. Davison, A., "Basic Neurochemistry: Molecular, Cellular, and Medical Aspects," *Journal of neurology, neurosurgery, and psychiatry*, Vol. 52, no. 8, p. 1021, 1989.

18. Schmidt, C. E., and J. B. Leach, "Neural tissue engineering: Strategies for repair and regeneration," *Annual Review of Biomedical Engineering*, Vol. 5, pp. 293–347, 2003.

19. Verkhratsky, A., and A. Butt, *Glial Neurobiology: A Textbook*, 2007.

20. Katzung, B. G., S. B. Masters, and A. J. Trevor, *Basic and Clinical Pharmacology*, 2009.

21. Madura, T., "Pathophysiology of Peripheral Nerve Injury," pp. 1–10, 2004.

22. Arslantunali, D., T. Dursun, D. Yucel, N. Hasirci, and V. Hasirci, "Peripheral nerve conduits: Technology update," 2014.

23. Frostick, S. P., Q. Yin, and G. J. Kemp, "Schwann cells, neurotrophic factors, and peripheral nerve regeneration," *Microsurgery*, Vol. 18, pp. 397–405, 1998.

24. Topp, K. S., and B. S. Boyd, "Structure and biomechanics of peripheral nerves: nerve responses to physical stresses and implications for physical therapist practice.," *Physical therapy*, Vol. 86, no. 1, pp. 92–109, 2006.

25. Faroni, A., S. A. Mobasseri, P. J. Kingham, and A. J. Reid, "Peripheral nerve regeneration: Experimental strategies and future perspectives," *Advanced Drug Delivery Reviews*, Vol. 82, pp. 160–167, 2015.

26. Torigoe, K., H. F. Tanaka, a. Takahashi, a. Awaya, and K. Hashimoto, "Basic behavior of migratory Schwann cells in peripheral nerve regeneration.," *Experimental neurology*, Vol. 137, no. 2, pp. 301–308, 1996.

27. Li, R., Z. Liu, Y. Pan, L. Chen, Z. Zhang, and L. Lu, "Peripheral Nerve Injuries Treatment: A Systematic Review," *Cell Biochemistry and Biophysics*, Vol. 68, no. 3, pp. 449–454, 2014.

28. Tabesh, H., G. Amoabediny, N. S. Nik, M. Heydari, M. Yosefifard, S. O. R. Siadat, and K. Mottaghy, "The role of biodegradable engineered scaffolds seeded with Schwann cells for spinal cord regeneration.," *Neurochemistry international*, Vol. 54, pp. 73–83, feb 2009.

29. Angius, D., H. Wang, R. J. Spinner, Y. Gutierrez-Cotto, M. J. Yaszemski, and A. J. Windebank, "A systematic review of animal models used to study nerve regeneration in tissue-engineered scaffolds," *Biomaterials*, Vol. 33, no. 32, pp. 8034–8039, 2012.

30. Subramanian, A., U. M. Krishnan, and S. Sethuraman, "Fabrication, characterization and in vitro evaluation of aligned PLGA-PCL nanofibers for neural regeneration," *Annals of Biomedical Engineering*, Vol. 40, no. 10, pp. 2098–2110, 2012.

31. Gu, X., F. Ding, Y. Yang, and J. Liu, "Construction of tissue engineered nerve grafts and their application in peripheral nerve regeneration," *Progress in Neurobiology*, Vol. 93, no. 2, pp. 204–230, 2011.

32. Ige, O. O., L. E. Umoru, and S. Aribo, "Natural Products: A Minefield of Biomaterials," *ISRN Materials Science*, Vol. 2012, pp. 1–20, 2012.

33. Cao, H., T. Liu, and S. Y. Chew, "The application of nanofibrous scaffolds in neural tissue engineering," *Advanced Drug Delivery Reviews*, Vol. 61, no. 12, pp. 1055–1064, 2009.

34. Vroman, I., and L. Tighzert, "Biodegradable polymers," *Materials*, Vol. 2, no. 2, pp. 307–344, 2009.

35. Chen, J.-P., and C.-H. Su, "Surface modification of electrospun PLLA nanofibers by plasma treatment and cationized gelatin immobilization for cartilage tissue engineering," *Acta Biomaterialia*, Vol. 7, no. 1, pp. 234–243, 2011.

36. Eling, B., S. Gogolewski, and A. J. Pennings, "Biodegradable materials of poly(l-lactic acid): 1. Melt-spun and solution-spun fibres," *Polymer*, Vol. 23, no. 11, pp. 1587–1593, 1982.

37. Bressan, E., L. Ferroni, C. Gardin, L. Sbricoli, L. Gobbato, F. Ludovichetti, I. Tocco, A. Carraro, A. Piattelli, and B. Zavan, "Graphene based scaffolds effects on stem cells commitment.," *Journal of translational medicine*, Vol. 12, no. 1, p. 296, 2014.

38. Seabra, A. B., A. J. Paula, R. de Lima, O. L. Alves, and N. Duran, "Nanotoxicity of Graphene and Graphene Oxide," *Chemical Research in Toxicology*, Vol. 27, no. 2, pp. 159–168, 2014.

39. Kiew, S. F., L. V. Kiew, H. B. Lee, T. Imae, and L. Y. Chung, "Assessing biocompatibility of graphene oxide-based nanocarriers: A review," *Journal of Controlled Release*, Vol. 226, pp. 217–228, 2016.

40. Li, J., X. Zeng, T. Ren, and E. van der Heide, "The Preparation of Graphene Oxide and Its Derivatives and Their Application in Bio-Tribological Systems," *Lubricants*, Vol. 2, pp. 137–161, 2014.

41. Chiu, N., T. Huang, and H. Lai, "Graphene Oxide Based Surface Plasmon Resonance Biosensors," 2013.

42. Tu, Q., L. Pang, Y. Chen, Y. Zhang, R. Zhang, B. Lu, and J. Wang, "Effects of surface charges of graphene oxide on neuronal outgrowth and branching.," *The Analyst*, Vol. 139, pp. 105–15, 2014.

43. Perreault, F., A. F. de Faria, S. Nejati, and M. Elimelech, "Antimicrobial Properties of Graphene Oxide Nanosheets: Why Size Matters," *ACS Nano*, no. 7, p. 150619235210004, 2015.

44. Hoppen, H. J., J. W. Leenslag, A. J. Pennings, B. van der Lei, and P. H. Robinson, "Two-ply biodegradable nerve guide: basic aspects of design, construction and biological performance," *Biomaterials*, Vol. 11, no. 4, pp. 286–290, 1990.

45. Schlosshauer, B., E. Müller, B. Schröder, H. Planck, and H. W. Müller, "Rat Schwann cells in bioresorbable nerve guides to promote and accelerate axonal regeneration," *Brain Research*, Vol. 963, no. 1-2, pp. 321–326, 2003.

46. Bini, T. B., S. Gao, X. Xu, S. Wang, S. Ramakrishna, and K. W. Leong, "Peripheral nerve regeneration by microbraided poly(L-lactide-co-glycolide) biodegradable polymer fibers.," *Journal of biomedical materials research. Part A*, Vol. 68, no. 2, pp. 286–295, 2004.

47. Uebersax, L., M. Mattotti, M. Papaloïzos, H. P. Merkle, B. Gander, and L. Meinel, "Silk fibroin matrices for the controlled release of nerve growth factor (NGF)," *Biomaterials*, Vol. 28, no. 30, pp. 4449–4460, 2007.

48. Dalton, P. D., L. Flynn, and M. S. Shoichet, "Manufacture of poly(2-hydroxyethyl methacrylate-co-methyl methacrylate) hydrogel tubes for use as nerve guidance channels," *Biomaterials*, Vol. 23, no. 18, pp. 3843–3851, 2002.

49. Koppes, R. A., S. Park, T. Hood, X. Jia, N. Abdolrahim Poorheravi, A. H. Achyuta, Y. Fink, and P. Anikeeva, "Thermally drawn fibers as nerve guidance scaffolds," *Biomaterials*, Vol. 81, pp. 27–35, 2016.

50. Rampichova, M., M. Buzgo, J. Chvojka, E. Prosecka, O. Kofronova, and E. Amler, "Cell penetration to nanofibrous scaffolds: Forcespinning, an alternative approach for fabricating 3D nanofibers," 2014.

51. Greiner, A., and J. H. Wendorff, "Electrospinning: A fascinating method for the preparation of ultrathin fibers," *Angewandte Chemie - International Edition*, Vol. 46, no. 30, pp. 5670–5703, 2007.

52. Doshi, J., and D. Reneker, "Electrospinning process and applications of electrospun fibers," *Conference Record of the 1993 IEEE Industry Applications Conference Twenty-Eighth IAS Annual Meeting*, Vol. 35, pp. 151–160, 1993.

53. Li, Z., and C. Wang, "One-Dimensional nanostructures," pp. 15–29, 2013.

54. Sill, T. J., and H. A. von Recum, "Electrospinning: Applications in drug delivery and tissue engineering," *Biomaterials*, Vol. 29, no. 13, pp. 1989–2006, 2008.

55. Bhardwaj, N., and S. C. Kundu, "Electrospinning: A fascinating fiber fabrication technique," *Biotechnology Advances*, Vol. 28, no. 3, pp. 325–347, 2010.

56. Pillay, V., C. Dott, Y. E. Choonara, C. Tyagi, L. Tomar, P. Kumar, L. C. Du Toit, and V. M. K. Ndesendo, "A review of the effect of processing variables on the fabrication of electrospun nanofibers for drug delivery applications," *Journal of Nanomaterials*, Vol. 2013, 2013.

57. Zander, N. E., "Hierarchically structured electrospun fibers," *Polymers*, Vol. 5, no. 1, pp. 19–44, 2013.

58. Ku, S. H., and C. B. Park, "Myoblast differentiation on graphene oxide," *Biomaterials*, Vol. 34, no. 8, pp. 2017–2023, 2013.

59. Mattanavee, W., O. Suwantong, S. Puthong, T. Bunaprasert, V. P. Hoven, and P. Supaphol, "Immobilization of biomolecules on the surface of electrospun polycaprolactone fibrous scaffolds for tissue engineering," *ACS Applied Materials and Interfaces*, Vol. 1, no. 5, pp. 1076–1085, 2009.

60. Qin, C.-C., X.-P. Duan, L. Wang, L.-H. Zhang, M. Yu, R.-H. Dong, X. Yan, H.-W. He, and Y.-Z. Long, "Melt electrospinning of poly(lactic acid) and polycaprolactone microfibers by using a hand- operated Wimshurst generator," *Nanoscale*, pp. 16611–16615, 2015.

61. Suzuki, T., A. Ei, Y. Takada, H. Uehara, T. Yamanobe, and K. Takahashi, "Modification of physical properties of poly(l-lactic acid) by addition of methyl-β-cyclodextrin," *Beilstein Journal of Organic Chemistry*, Vol. 10, pp. 2997–3006, 2014.

62. Wesełucha-Birczyńska, A., A. Frączek-Szczypta, E. Długoń, K. Paciorek, A. Bajowska, A. Kościelna, and M. Błażewicz, "Application of Raman spectroscopy to study of the polymer foams modified in the volume and on the surface by carbon nanotubes," *Vibrational Spectroscopy*, Vol. 72, pp. 50–56, 2014.

63. Yan, J.-l., G.-j. Chen, J. Cao, W. Yang, B.-h. Xie, and M.-b. Yang, "Functionalized graphene oxide with ethylenediamine and 1,6-hexanediamine," *New Carbon Materials*, Vol. 27, no. 5, pp. 370–376, 2012.

64. Gao, W., "The chemistry of graphene oxide," *Graphene Oxide: Reduction Recipes, Spectroscopy, and Applications*, pp. 61–95, 2015.

65. Johra, F. T., J. W. Lee, and W. G. Jung, "Facile and safe graphene preparation on solution based platform," *Journal of Industrial and Engineering Chemistry*, Vol. 20, no. 5, pp. 2883–2887, 2014.

66. De Luca, A. C., J. S. Stevens, S. L. M. Schroeder, J. B. Guilbaud, A. Saiani, S. Downes, and G. Terenghi, "Immobilization of cell-binding peptides on poly-e-caprolactone film surface to biomimic the peripheral nervous system," *Journal of Biomedical Materials Research - Part A*, Vol. 101 A, no. 2, pp. 491–501, 2013.

67. Rangappa, N., A. Romero, K. D. Nelson, R. C. Eberhart, and G. M. Smith, "Laminin-coated poly(L-lactide) filaments induce robust neurite growth while providing directional orientation," *Journal of Biomedical Materials Research*, Vol. 51, no. 4, pp. 625–634, 2000.

68. Ranjbar-Mohammadi, M., M. P. Prabhakaran, S. H. Bahrami, and S. Ramakrishna, "Gum tragacanth/poly(l-lactic acid) nanofibrous scaffolds for application in regeneration of peripheral nerve damage," *Carbohydrate Polymers*, Vol. 140, pp. 104–112, 2016.

69. Zong, X., K. Kim, D. Fang, S. Ran, B. S. Hsiao, and B. Chu, "Structure and process relationship of electrospun bioabsorbable nanofiber membranes," *Polymer*, Vol. 43, no. 16, pp. 4403–4412, 2002.

70. Zafar, M., S. Najeeb, Z. Khurshid, M. Vazirzadeh, S. Zohaib, B. Najeeb, and F. Sefat, "Potential of electrospun nanofibers for biomedical and dental applications," 2016.

71. Hsu, C. M., and S. Shivkumar, "N,N-dimethylformamide additions to the solution for the electrospinning of poly(ϵ-caprolactone) nanofibers," *Macromolecular Materials and Engineering*, Vol. 289, no. 4, pp. 334–340, 2004.

72. Kolbuk, D., P. Sajkiewicz, K. Maniura-Weber, and G. Fortunato, "Structure and morphology of electrospun polycaprolactone/gelatine nanofibres," in *European Polymer Journal*, Vol. 49, pp. 2052–2061, 2013.

73. Pinto, A. M., J. Cabral, D. A. P. Tanaka, A. M. Mendes, and F. D. Magalhaes, "Effect of incorporation of graphene oxide and graphene nanoplatelets on mechanical and gas permeability properties of poly(lactic acid) films," *Polymer International*, Vol. 62, no. 1, pp. 33–40, 2013.

74. Tong, Y., Y. Lin, S. Wang, and M. Song, "A study of crystallisation of poly (ethylene oxide) and polypropylene on graphene surface," *Polymer*, Vol. 73, pp. 52–61, 2015.

75. Zhu, Y., C. Gao, X. Liu, T. He, and J. Shen, "Immobilization of biomacromolecules onto aminolyzed poly(L-lactic acid) toward acceleration of endothelium regeneration.," *Tissue engineering*, Vol. 10, no. 1, pp. 53–61, 2004.

76. Jung, H. S., M.-Y. Lee, W. H. Kong, I. H. Do, and S. K. Hahn, "Nano Graphene Oxide Hyaluornic Acid Conjugate for Target Specific Cancer Drug Delivery," *RSC Advances*, pp. 14197–14200, 2014.

77. Jing, X., H. Y. Mi, M. R. Salick, X. F. Peng, and L. S. Turng, "Preparation of thermoplastic polyurethane/graphene oxide composite scaffolds by thermally induced phase separation," *Polymer Composites*, Vol. 35, no. 7, pp. 1408–1417, 2014.

78. Xu, Y., W. Hong, H. Bai, C. Li, and G. Shi, "Strong and ductile poly(vinyl alcohol)/graphene oxide composite films with a layered structure," *Carbon*, Vol. 47, no. 15, pp. 3538–3543, 2009.

79. Zhang, K., H. Zheng, S. Liang, and C. Gao, "Aligned PLLA nanofibrous scaffolds coated with graphene oxide for promoting neural cell growth," *Acta Biomaterialia*, Vol. 37, pp. 131–142, 2016.